The Microtubule-Associated Protein END BINDING1b, Auxin, and Root Responses to Mechanical Cues

by

Shannon Squires

B.Sc., Simon Fraser University, 2008

Thesis Submitted in Partial Fulfillment
of the Requirements for the Degree of
Master of Science

in the
Department of Biological Sciences
Faculty of Science

SIMON FRASER UNIVERSITY

Summer 2013

Approval

Name: **Shannon Squires**

Degree: **Master of Science (Biological Sciences)**

Title of Thesis: ***The Microtubule-Associated Protein END BINDING1b, Auxin, and Root Responses to Mechanical Cues***

Examining Committee:

Chair: David Lank, Adjunct Professor

Sherryl Bisgrove
Senior Supervisor
Associate Professor

Jim Mattsson
Supervisor
Associate Professor

Lynne Quarmby
Supervisor
Professor

Allison Kermode
Internal Examiner
Professor
Department or Biology

Date Defended/Approved: April 26, 2013

Partial Copyright Licence

Abstract

The microtubule associated protein END BINDING1b (EB1b) is a regulator of root responses to mechanical cues. Here, three studies aimed at understanding the role of EB1b in these processes are presented. First, the relationship between EB1b and auxin during root responses to mechanical cues was assessed. The results suggest that EB1b and auxin transport/signaling affect root responses by different mechanisms. Next, the effects of altered EB1b expression levels and protein structure on root responses were investigated. Overexpression of EB1b reduced root responses, and the addition of GFP to the carboxy terminus of the protein abolished its ability to act as a repressor. Finally, evidence was obtained that supports a model in which root responses to mechanical cues are modulated by two competing processes, one activating and one repressing. In this model, repression by EB1b would provide a threshold which touch stimulation must overcome to elicit a response.

Keywords: EB1; Cytoskeleton; Mechanical Cues; Auxin; Root Growth

Table of Contents

Approval ii
Partial Copyright Licence iii
Abstract iv
Table of Contents v
List of Figures vii
List of Tables viii

1. Introduction 1
1.1. Root responses to gravity 2
1.2. Root responses to touch 3
1.3. Auxin 4
1.4. END BINDING1 5
1.5. References 6

2. The Microtubule-Associated Protein End Binding1b, Auxin, and Root Responses to Mechanical Cues 8
2.1. Introduction 8
2.2. Materials and Methods 11
2.2.1. Plant Materials and Growth Conditions 11
2.2.2. Genotyping 12
2.2.3. Phenotypic and Statistical Analyses 12
2.3. Results 13
2.3.1. eb1b-1 Roots are Hypersensitive to Reductions in Auxin Transport 15
2.3.2. NPA Reduces Auxin Transport by Equivalent Amounts in eb1b-1 and Wild Type Roots 18
2.3.3. Auxin Signaling Modulates Loop Formation in Roots 19
2.3.4. Effects of IAA, NAA and 2, 4-D on Root Responses to Mechanical Cues 20
2.4. Discussion 24
2.5. References 27

3. Repression of root responses to mechanical cues by EB1b: Examining the effects of overexpression and of GFP fusions to the C-terminal tail. 31
3.1. Introduction 31
3.2. Methods and Materials 32
3.2.1. Plant material and culture conditions 32
3.2.2. Phenotypic analyses 33
3.2.3. Extraction of nucleic acids and quantification of relative EB1b expression levels 33
3.3. Results: 34
3.3.1. Root growth analyses of wild type, eb1b-1 mutants, and transgenic lines 35

3.3.2. Root responses to mechanical cues are correlated with EB1b expression level 38
3.3.3. EB1b-GFP fusions are functionally impaired 40
3.4. Discussion 43
3.5. References 44

4. The Microtubule Associated Protein END BINDING1 Represses Root Responses to Mechanical Cues 47
4.1. Introduction 47
4.2. Materials and methods 50
4.2.1. Plant material and growth conditions 50
4.2.2. Phenotypic and Statistical Analyses 51
4.2.3. Extraction of nucleic acids 51
4.2.4. Genotyping 52
4.3. Results 53
4.3.1. eb1b-1 mutants are hypersensitive to increases in mechanical stimulation 53
4.3.2. eb1b-1 roots have delayed responses to gravity when grown inside the agar 54
4.3.3. Double mutant analyses 55
4.3.4. Root responses to mechanical cues in eb1b-1 pgm-1 double mutants 56
4.3.5. Analyses of eb1b-1 arg1-3 double mutants 56
4.3.6. Molecular characterization of T-DNA insertional alleles of TCH3 57
4.3.7. Gravitropic response of tch3-1 when grown inside the agar 58
4.3.8. tch3-1 mutants are resistant to mechanical cues 59
4.4. Discussion 60
4.4.1. EB1b represses root responses to mechanical cues 60
4.4.2. Genetic interactions between EB1b and components of gravity and touch signaling pathways. 61
4.4.3. Roles for EB1b in root responses to touch/gravity cues: A model 62
4.5. References 70

5. Conclusion 75

List of Figures

Figure 2.1. Both eb1b-1 and auxin transport mutants have roots that form more loops than wild type plants when grown on reclined agar plates. 14

Figure 2.2. Roots of eb1b-1 mutants are hypersensitive to the auxin transport inhibitor NPA. 16

Figure 2.3. Roots of eb1b-1 mutants are more sensitive than wild type to TIBA. 17

Figure 2.4. NPA affects auxin transport equivalently in eb1b-1 and Ws roots. 19

Figure 2.5. Roots of eb1b-1 mutants exhibit an enhanced and sustained sensitivity to PCIB. 20

Figure 2.6. Effects of IAA on root responses to mechanical cues. 22

Figure 2.7. Effects of NAA on root responses to mechanical cues. 23

Figure 2.8. 2, 4-D reduces root responses to mechanical cues. 24

Figure 3.1. EB1b expression levels relative to APT1 in wild type and transgenic eb1b-1 lines. 35

Figure 3.2. Phenotypes of roots responding to combinations of mechanical cues and gravity. 37

Figure 3.3. Quantification of root responses to touch/gravity stimulation in transgenic eb1b-1 mutants expressing EB1b constructs. 39

Figure 3.4. Quantification of root responses to touch/gravity stimulation in transgenic eb1b-1 mutants expressing EB1b-GFP constructs. 41

Figure 3.5. EB1b-GFP localizes to growing MT ends. 42

Figure 4.1. The roots of eb1b-1 mutants are more sensitive to growth on reclined agar plates than Ws or eb1b-1 transformed with an EB1b construct (eb1b-1 pEB1b:EB1b). 64

Figure 4.2. Gravitropic responses of eb1b-1 mutants and wild type when grown through an agar medium. 65

Figure 4.3. Phenotypic analyses of eb1b-1 pgm-1 double mutants. 66

Figure 4.4. Eb1b-1 arg1-3 double mutant roots skewed and looped less than eb1b-1. 67

Figure 4.5. RT-PCR analysis of TCH3 T-DNA insertional lines. 68

Figure 4.6. Phenotypic analysis of tch3-1 and eb1b-1 tch3-1 seedlings. 69

Figure 5.1. A model for the roles of EB1b, auxin, and TCH3 in responses to mechanical cues 75

Figure 5.2. A model for the activity of EB1b at the MT plus end. 76

List of Tables

Table 3.1. A comparison of microtubule growth rates 43

1. Introduction

Plants are anchored into the soil by their roots and remain at one site for the duration of their lives. Because the environment around them changes continuously, plants are exposed to a wide range of environmental stimuli. To respond to these environmental cues, plants alter their patterns of growth. Gravity and touch are two constant cues that shape the growth of plants. Gravity directs roots down into the ground where they seek out moisture and nutrients. In terms of touch, roots receive mechanical stimulation from the soil and rocks around them. Roots must navigate through a complex, heterogeneous environment, avoiding obstacles that may impede their growth. If a root encounters an obstacle, it must modify its patterns of cell division and expansion to alter the direction of its growth.

In roots, growth occurs in two specialized regions: the meristem and elongation zone. The meristem, at the tip of the root, contains actively dividing cells that continually produce new cells to increase the width and length of the root. Farther back towards the base of the root is the elongation zone (EZ) where cells expand anisotropically, along the length of the root. The expansion of cells in the EZ increases the length of the root and pushes the tip forward. As the root tip moves through the environment, it may encounter an obstacle. To grow around the obstacle, the root must alter its trajectory, and grow in a new direction. For this to occur successfully, the plant downregulates its response to gravity (Massa and Gilroy 03).

To succeed in the environment, plants must monitor and respond to combinations of touch and gravity. The pathways regulating responses to these two types of stimuli engage in cross-talk with each other. Plant responses to gravity stimulation have been studied extensively. In contrast, whereas some of the molecular components involved in regulating root responses to touch have been identified, the mechanisms involved in the detection of mechanical stimuli are not well understood.

1.1. Root responses to gravity

Roots detect changes in their position relative to gravity in the root cap, and a signal is sent from the site of detection to cells in the elongation zone which then respond by forming a bend. The response to gravity is divided into three phases: perception, signal transduction, and differential growth. First, a change in orientation relative to gravity must be detected, and translated into a chemical signal. The detection of gravity occurs in specialized cells within the root cap, the columella. Columella cells contain starch-filled plastids called amyloplasts that sediment to the bottom of the cells. When roots are reoriented relative to gravity, amyloplasts fall to the new bottom and this movement is detected in the columella cell by an unknown mechanism. Mutant plants lacking columella cells and/or amyloplasts have reduced ability to respond to gravity (Blancaflor et al. 1998). Amyloplast settling does not appear to be the only way by which plant cells can detect gravity. There are mutants which are unable to synthesize starch (*phosphoglucomutase* or *pgm*) yet they still exhibit a gravitropic response, albeit in an incomplete form (Caspar and Pickard, 1989). Another model that has been put forward to explain how plant cells could detect gravity is known as the protoplast pressure model (Staves, 1997). It postulates that cells can detect the direction of gravity because of differences in tension and compression at the protoplast/cell wall interface. The weight of the protoplast would exert tension on the upper side of the cell and compression on the lower and these differences are somehow detected by the cell. After the gravity stimulus has been detected, a signal is transmitted to the elongation zone to initiate a growth response. The signal that moves from the root cap to the EZ is the plant hormone, auxin.

Auxin is synthesized in developing tissues (Ljung et al, 2001), and is transported polarly throughout the plant, moving from shoots, through the vascular tissue, towards the tip of the root. When auxin reaches the tip of a vertically oriented root it is redirected laterally and uniformly transported towards the elongation zone (Michniewicz, 2007). In a gravistimulated root that has been oriented horizontally, however, the direction of auxin flow through the root tip is concentrated to the lower flank of the root, resulting in an auxin gradient. The high concentration of auxin in the lower flank causes a decrease in

cell expansion relative to the upper flank (Mullen et al, 1998). The resulting differential growth rates across the root cause the root to bend down.

1.2. Root responses to touch

In contrast to the knowledge on plant responses to gravity, information on their responses to touch is lacking. This paucity exists because it is often difficult to separate the two stimuli. Acknowledging the interconnectedness of touch and gravity, a common assay is used to study various combinations of the stimuli. This involves growing plants on the surface of agar petri plates reclined at different angles (Okada and Shimura, 1990). On vertically oriented plates, seedlings receive only a mild touch stimulus from the surface. In this orientation, gravity is the main stimulus presented to the plant, and root growth proceeds downwards in a relatively straight trajectory. If the agar plate is reclined, the root tip attempts to grow down but it encounters the agar surface more frequently. The increased interaction between the root and agar surface results in complex growth patterns; roots skew to the left, wave back and forth, and form loops. These growth patterns are thought to develop as a consequence of positive gravitropism and root interactions with the agar surface (Thompson and Holbrook, 2004).

Root growth assays on reclined agar plates have identified an array of proteins and molecular components that mediate responses to combinations of touch and gravity. The key proteins include those which act in modifying cell walls, microtubule function and/or organization, and signalling pathways. Other molecular components include protons, plant hormones, Ca^{2+} and reactive oxygen species. (Vaughn et al, 2011) From this list I focused on the microtubule associated protein END BINDING1 (EB1) and the plant hormone auxin, specifically, the role of EB1 in root responses to combinations of mechanical cues and gravity, and how it may interact with auxin in these responses. In the following two sections I provide background on the role of auxin and EB1.

1.3. Auxin

The hormone, auxin, is transported polarly throughout the plant. Cells regulate the directional movement of auxin in part because of its chemical nature. The endogenous form of auxin, indole acetic acid (IAA), is a weak acid. Outside of the cell, in the acidic environment of the apoplast, the majority of IAA exists in a protonated, neutral state, and a small proportion of IAA is dissociated. The uncharged, lipophilic IAA molecule can pass through the cell membrane by diffusion (Rubery and Sheldrake, 1974); however, the ionic form requires the assistance of an influx carrier to enter the cell. Transporter-mediated import of auxin is carried out by members of the AUXIN RESISTANT1 (AUX1) /LIKE-AUX1 (LAX) protein family (Bennett et al. 1996). Once inside the cell, IAA dissociates, and in an ionized state, can no longer diffuse through the membrane. Auxin export from cells is mediated by efflux carriers such as PIN-FORMED (PIN) proteins (Petrasek et al. 2006) or P-GLYCOPROTEIN ABC transporters (Geisler and Murphy 2006). Auxin transport proteins are polarly localized within cells, and their localization correlates with the direction of auxin flow (Wisniewska et al, 2006). Plants are able to alter the direction of auxin flow and generate local gradients by relocalizing these transporters. The formation of auxin gradients precedes many growth responses, such as during a gravitropic bend.

One way that auxin functions in cells is by altering gene expression through the degradation of transcriptional repressors (Aux/IAA proteins) (Parry and Estelle, 2006). In the absence of auxin, Aux/IAA repressors inhibit gene expression by dimerizing with Auxin Response Factor (ARF) transcription factors. Repression is relieved by degradation of Aux/IAAs in the presence of auxin. When auxin is present, it is perceived by a family of receptors: TRANSPORT INHIBITOR RESPONSE 1 (TIR1)/AUXIN F-BOX PROTEINs (AFBs) (Kepinski and Leyser, 2005; Dharmasiri et al, 2005). The binding of auxin to one of these receptors initiates the recruitment of Aux/IAA repressors to the complex. This in turn targets the repressors to the proteasome for degradation, thereby relieving the inhibition of gene expression. Auxin mediated gene expression is important during gravitropic responses, as quadruple *tir1/afb* mutants exhibit agravitropic phenotypes (Dharmasiri et al, 2005b). Many genes are rapidly upregulated in response

to auxin; however, the mechanisms by which gene expression results in altered growth responses in the root are not well understood.

1.4. END BINDING1

EB1 is a highly conserved microtubule associated protein (MAP) that localizes to the plus ends of growing microtubules (MT). EB1 proteins transiently bind and dissociate from the tip as the MT grows through the cytoplasm. In animal and fungal cells, EB1 is involved in regulating microtubule dynamics; it promotes polymerization and prevents destabilization (Akhmanova and Steinmetz, 2008). EB1 has also been found to interact with a wide array of proteins and is thought to function as part of a complex at the plus-end of the MT.

In plants, less is known about the function of EB1. In the *Arabidopsis thaliana* genome there are 3 EB1 genes: *EB1a*, *EB1b*, and *EB1c*. Plants carrying T-DNA insertions in each of these genes have been isolated and have defects in responding to mechanical cues. Mutations in *EB1b* show the most severe phenotype. When grown on assays that provide mechanical stimulation, the roots of *eb1b* mutants skew to the left and form loops. In contrast, wild type roots grow relatively straight. The increased sensitivity to touch suggests that EB1 is a repressor of responses to mechanical cues.

In this thesis I examine some of the molecular mechanisms by which roots respond to combinations of mechanical cues and gravity. Specifically, my project focuses on the relationship between EB1b, auxin, and touch. In chapter 2 I investigate a possible interaction between auxin and EB1 in root responses to mechanical cues. This work forms the main component of my thesis. Chapter 3 is a collaborative effort between several members in the lab. I mentored Doris Cheng, an undergraduate, and together we conducted and analyzed all the root growth assays shown in the chapter. I also collaborated with Vita Lai, Saeid Shahidi, and Sachini Ariyaratne to determine expression levels of EB1 in transgenic plants, EB1b-GFP localization patterns, and microtubule growth rates. Chapter 4 examines the interaction between *EB1b* and other genes involved in touch and gravity. I contributed the data showing that an EB1b

construct rescues the *eb1b-1* mutant phenotype, I assessed the elongation rates of various mutant roots, and showed that the *tch3-1* allele is recessive.

1.5. References

. Akhmanova A, Steinmetz MO (2010) Microtubule +TIPs at a glance. J Cell Sci 123:3415-3419.

Benková E, Michniewicz M, Sauer M, Teichmann T, Seifertová D, Jürgens G, Friml J (2003) Local, efflux-dependent auxin gradients as a common module for plant organ formation. Cell 115:591-602.

Bennett MJ, Marchant A, Green HG, May ST, Ward SP, Millner PA, Walker AR, Schulz B, Feldmann KA (1996) Arabidopsis AUX1 gene: a permease-like regulator of root gravitropism. Science 273:948–950.

Blancaflor EB., Fasano J, and Gilroy S (1998) Mapping the functional roles of cap cells in the response of Arabidopsis primary roots to gravity. Plant Physiology 116:213-23.

Dharmasiri N, Dharmasiri S, Weijers D, Lechner E, Yamada M, Hobbie L, Ehrismann JS, Jürgens G, Estelle M (2005) Plant development is regulated by a family of auxin receptor F box proteins. Dev Cell 9(1):109-119.

Dharmasiri, N, Dharmasiri, S, and Estelle, M (2005b) The F-box protein TIR1 is an auxin receptor. Nature 435(7041):441–445.

Geisler M, Murphy AS (2006) The ABC of auxin transport: the role of p-glycoproteins in plant development. FEBS Lett 580:1094–1102.

Kepinski S, Leyser O (2005) The Arabidopsis F-box protein TIR1 is an auxin receptor. Nature 4355(1):446–451.

Ljung K, Bhalerao RP, Sandberg G (2001) Sites and homeostatic control of auxin biosynthesis in Arabidopsis during vegetative growth. Plant J 285(1):465–74.

Marchant A, Kargul J, May ST, Muller P, Delbarre A, Perrot-Rechenmann C, Bennett MJ (1999) AUX1 regulates root gravitropism in Arabidopsis by facilitating auxin uptake within root apical tissues. EMBO J 185(1):2066–2073.

Massa Gand Gilroy S (2003) Touch modulates gravity sensing to regulate the growth ofprimary roots of Arabidopsis thaliana. The Plant Journal 33(3):435–445.

Michniewicz M, Brewer PB, Friml J (2007) Polar auxin transport and asymmetric auxin distribution. The Arabidopsis Book 5:1–28.

Mullen J, Ishikawa H, Evans ML (1998) Analysis of changes in relative elemental growth rate patterns in the elongation zone of Arabidopsis roots upon gravistimulation. Planta 206:598-603.

Okada K, Shimura Y (1990) Reversible root tip rotation in Arabidopsis seedlings induced by obstacle-touching stimulus. Science 250:274-276.

Parry G, Estelle M (2006) Auxin receptors: a new role for F-box proteins. Curr Opin Cell Biol18(2):152-6.

Petrásek J, Mravec J, Bouchard R, Blakeslee JJ, Abas M, Seifertová D, Wisniewska J, Tadele Z, Kubes M, Covanová M, Dhonukshe P, Skupa P, Benková E, Perry L, Krecek P, Lee OR, Fink GR, Geisler M, Murphy AS, Luschnig C, Zazímalová E, Friml J (2006) PIN proteins perform a rate-limiting function in cellular auxin efflux. Science 312:914–918.

Rubery PH, Sheldrake AR (1974) Carrier-mediated auxin transport. Planta 118:101–121.

Staves MP 1997. Cytoplasmic streaming and gravity sensing in Chara internodal cells. Planta 203:S79-S84.

Thompson MV, Holbrook NM (2004) Root-gel interactions and the root waving behavior of Arabidopsis. Plant Physiol 135:1822-1837.

Vaughn LM, Baldwin KL, Jia G, Verdonk JC, Strohm AK, Masson PH (2011) The cytoskeleton and root growth behavior. In: Liu B (ed) Advances in Plant Biology, vol 1. The Plant Cytoskeleton. Springer, New York, pp 307-326.

Wisniewska J, Xu J, Seifertová D, Brewer PB, Ruzicka K, Blilou I, Rouquié D, Benková E, Scheres B, Friml (2006) Polar PIN localization directs auxin flow in plants. J.Science 312(5775):883.

2. The Microtubule-Associated Protein End Binding1b, Auxin, and Root Responses to Mechanical Cues

A version of this chapter has been published in The Journal of Plant Growth Regulation (April 2013). Authors include Shannon Squires and Sherryl Bisgrove.

2.1. Introduction

The primary function of the root system is to provide surfaces across which water and nutrients are absorbed. To fulfill this role, roots are able to penetrate through the soil and direct their growth into areas where conditions are optimal. Growth is generally directed downwards in response to gravity, although this growth direction is often modified as the root senses and responds to the signals it receives from its surroundings. Mechanical cues represent one signal that roots continuously monitor and respond to as they force their way through areas of differing densities in the soil and wind around rocks and other impediments. The ability of roots to sense and respond appropriately to multiple levels of mechanical stimulation requires an ability to modulate output from mechanosensory response systems.

The mechanisms that underlie root responses to mechanical cues are an active area of investigation. Several molecular components involved in the response have been identified. These include Ca^{2+}, protons, reactive oxygen species, multiple plant hormones, and several proteins involved in signaling pathways, cell wall modification, and microtubule organization and/or function (for reviews see Monshausen and Gilroy 2009; Chehab et al. 2011; Vaughn et al. 2011). However, the interactions that occur between these factors in the regulatory network that controls root responses to touch are largely unknown.

Root responses to mechanical cues are often assessed by analyzing roots growing down along the surfaces of agar plates. This regime causes roots to grow in patterns that reflect their responses to touch and gravity stimulation. On plates reclined from a vertical orientation, gravitropism causes the root tip to press against the agar surface and the resulting mechanical cues cause roots to form waves and loops and to skew to one side as they grow (Rutherford and Masson 1996; Thompson and Holbrook 2004; Oliva and Dunand 2007; Migliaccio et al. 2009; Vaughn et al. 2011). Using this assay, several groups have identified mutants with altered root skewing and looping patterns (see Vaughn et al. 2011 for review). Seedlings carrying mutations in the proteins that control the movement of auxin into and out of cells as well as in the microtubule associated protein EB1b are examples of genotypes whose roots skew and loop more than wild type (Okada and Shimura 1990; Chen er al. 1998; Bisgrove et al. 2008; Gleeson and Bisgrove 2012).

The plant hormone auxin is a well-known regulator of root growth, development, and responses to environmental cues. In roots that are growing down, auxin is transported from the shoot to the root apex through the central cylinder where, in combination with *de novo* auxin synthesis, an auxin maxima is formed. From the root tip auxin flows laterally through the root cap and is then transported basipetally to the elongation zone through the cortical and epidermal cell layers. This flow of auxin establishes an auxin gradient along the root that maintains the stem cell niche in the meristem and regulates cell elongation (for review see Jones and Ljung 2012). When roots are rotated away from vertical, they respond by redirecting auxin flow across the root cap. More auxin moves to the bottom side of the root cap and its basipetal transport then leads to higher levels of auxin on the lower side of the root and reduced levels on the upper side. These changes in auxin concentrations alter cell elongation rates across the root; an increase on the upper flank and a decrease on the bottom causes the root to form a downward bend (reviewed in Friml 2010; Muday and Rahman 2008). Auxin flow is mediated by the AUXIN RESISTANT1 (AUX1) influx and PIN FORMED (PIN) efflux carriers, proteins that control the movement of auxin into and out of cells (Peer et al. 2011). Treatments or mutations that disrupt auxin transport reduce the ability of roots to respond to gravity and they increase loop formation in roots growing along an agar surface, suggesting that auxin transport is needed for gravitropism and to repress

looping in response to mechanical cues (Okada and Shimura 1990; Chen et al. 1998; Vaughn et al. 2011).

Microtubules represent another cellular component whose disruption alters root growth on agar surfaces. Treatments or mutations that alter microtubule organization and/or function can cause roots to twist as they grow. On agar surfaces, these excessively twisted roots also skew more than wild type untreated plants. In several mutants, a correlation has been observed between root twisting and the orientation of cortical microtubules in elongating cells. Twisted roots often have microtubules arranged in helical arrays positioned at oblique angles in elongating cells. According to one model, these obliquely oriented cortical microtubules cause cells to elongate at an angle rather than parallel with the long axis of the root, thereby causing the root to twist (Hashimoto 2011). Arabidopsis seedlings carrying mutations in the gene coding for the microtubule associated protein END BINDING 1b (EB1b) also have roots that skew and loop more than wild type. However, *eb1b* mutant roots are not excessively twisted and they have microtubule arrays that appear to be normal (Bisgrove et al. 2008). This phenotype indicates that EB1b and the proteins that are affected in mutants with twisted roots modulate looping and skewing in different ways, although the mechanism by which EB1b affects these root responses is unknown.

EB1b belongs to a large and diverse group of microtubule associated proteins known as microtubule plus end tracking proteins (or +TIPs), named because they preferentially associate with the more rapidly growing or plus ends of microtubules. +TIPs have been most intensively studied in animal and fungal cells and this work has shown that the group includes a diverse array of proteins that have many different functions in cells (Akhmanova and Steinmetz 2010). They include proteins that participate in signaling pathways, modify actin arrays, regulate microtubule growth and depolymerization (dynamics), and link microtubule ends with other cellular components (Sun et al. 2008; Liu et al. 2009; Akhmanova and Steinmetz 2010). EB1 family members are different from other +TIPs that have been studied in that they bind directly to microtubule ends and they also interact with many other proteins in cells (Honnappa et al. 2009). Because of their ability to interact with and recruit other proteins to microtubule ends, EB1 family members are thought to be core regulatory components of +TIP protein complexes.

Three genes encoding EB1 family members are present in the Arabidopsis genome (Bisgrove et al. 2004). These are designated *EB1a* (At3g47690)*, EB1b* (At5g62500)*,* and *EB1c* (At5g67270). EB1c is thought to function primarily during mitosis; it localizes to mitotic microtubule arrays in dividing cells and is sequestered in the nucleus during interphase (Dixit et al. 2006; Komaki et al. 2010). Although both EB1a and EB1b proteins preferentially accumulate on microtubule plus ends in mitotic and interphase cells, EB1b appears to play the predominant role during root responses to mechanical cues since the responses of *eb1b* single mutants are indistinguishable from homozygous *eb1a eb1b* double or *eb1a eb1b eb1c* triple mutants (Chan et al. 2003; Mathur et al. 2003; Van Damme et al. 2004; Dixit et al. 2006; Bisgrove et al. 2008; Gleeson et al 2012)

Here we assess a possible relationship between EB1b and auxin in the repression of root responses to mechanical cues. We find that the addition of chemicals that disrupt auxin transport enhance root responses to mechanical cues to a much greater extent in *eb1b-1* mutants than in wild type. The enhanced response of *eb1b-1* mutants was observed even though the auxin transport inhibitor NPA reduced auxin transport by equivalent amounts in mutant and wild type. We also found that the inhibition of auxin signaling enhanced the responses of roots to mechanical cues to a much greater extent in *eb1b-1* than it did in wild type. Taken together, these results suggest that EB1b and auxin transport/signaling affect root responses to mechanical cues in different ways.

2.2. Materials and Methods

2.2.1. Plant Materials and Growth Conditions

Wassilewskija (Ws), Columbia-0 (Col-0), *eir1-1*, *aux1-7*, and *DR5rev::GFP* seeds were obtained from The Arabidopsis Information Resource (TAIR; http://www.arabidopsis.org/). *eir1-1*, *aux1-7*, and *DR5rev::GFP* were all in a Col-0 background. The T-DNA insertional allele in the Ws accession *eb1b-1* was previously described by Bisgrove and others (2008). Unless otherwise stated, all chemicals were obtained from Sigma-Aldrich. Seeds were surfaced sterilized using the vapour phase

method (Clough and Bent 1998) and sown on 0.8% (w/v) Phytagar (Caisson Laboratories Inc.) plates containing half strength Murashige and Skoog (MS) supplemented with 1% (w/v) sucrose and 0.1% (w/v) 2-(N-morpholino) ethanesulfonic acid **(**MES) at pH 5.8. Seeds were vernalized in the dark at 4°C for 3 d and then grown at 20°C for 7 d under 16 h light/8 h dark conditions. Agar plates containing naphthylphthalamic acid (NPA), 2,3,5-triiodobenzoic acid (TIBA), *p*-chlorophenoxyisobutyric acid (PCIB), indole-3-acetic acid (IAA), 1-naphthaleneacetic acid (NAA), or 2, 4-dichlorophenoxyacetic acid **(**2, 4-D) were prepared by pipetting the appropriate amount of each chemical from concentrated dimethyl sulfoxide (DMSO) or ethanol stock solutions into molten agar. Control plates contained DMSO concentrations equal to the highest concentration in the plates with chemicals. *DR5rev::GFP* seedlings were grown on glass slides embedded in agar supplemented with varying concentrations of NPA.

2.2.2. Genotyping

Homozygous *eir1-1* seedlings were selected on the basis of their agravitropic phenotype from F2 progeny of crosses between *eb1b-1* and *eir1-1* (Rashotte et al., 2001). The genotypes of these seedlings at the *EB1b* locus were then determined by PCR. Seedlings carrying the wild type *Eb1b* allele were identified in a reaction using *Taq*DNA polymerase (Invitrogen) and the following primers (Forward 5'-GGTCATGCAAGAAGTCTTCACCAAATTGAA-3' and Reverse 5'-GCACAGATTCATTTGCATCGGTTGCGTA-3'). The primers *EB1b*F (5′-GCTTCTCCGTCCTTTTCTCTGCTTCAGTT-3′) and JL202 (5'-CATTTTATAATAACGCTGCGGACATCTAC-3′) confirmed the presence of the *eb1b-1* T-DNA insertion. Genomic DNA was extracted from whole seedlings as described previously (Dellaporta 1983).

2.2.3. Phenotypic and Statistical Analyses

Seedlings were photographed using an Olympus SZX16 stereo microscope equipped with a Retiga 4000R digital camera and QCapture Pro software. Slides with seedlings expressing the *DR5rev::GFP* construct were excised from the surrounding agar and imaged using an inverted Zeiss microscope and Hamamatsu 1394 ORCA-ERA

camera. Measurements were made from all images using ImageJ and statistical analyses were performed using JMP software. Two factor ANOVAs were used to compare responses of mutants and wild type seedlings to chemical treatments. Tukey's multiple comparison was used to test for differences between genotypes in the proportions of roots that formed loops on untreated agar plates.

2.3. Results

The responses of *eb1b-1* roots to mechanical cues were compared to those of two mutants with defects in auxin transport, *aux1-7* and *ethylene insensitive root1-1* (*eir1-1*). These seedlings have mutations in the genes that code for transporters that mediate auxin influx (*AUX1*) or efflux (*PIN2*) respectively from cells (Luschnig et al. 1998; Swarup et al. 2004). Both the *aux1* and *eir1-1* seedlings exist in the Col-0 genetic background while the *eb1b-1* allele is in Ws. We chose to analyze *eb1b-1* in the Ws background instead of *eb1b-2* seedlings (in Col-0) for two reasons: 1) Both wild type Ws and *eb1b-1* roots exhibit greater responses to mechanical cues than do Col-0 and *eb1b-2* seedlings (Bisgrove et al. 2008) and the reduced phenotype in the Col-0 genetic background greatly reduces our ability to detect statistically significant differences between the responses of *eb1b-2* mutants and wild type plants. 2) We have previously shown that expressing the *EB1b* gene in *eb1b-1* mutants restores root responses to that of wild type, providing evidence that, in the Ws genetic background, it is loss of EB1b alone that is responsible for the *eb1b-1* phenotype (Gleeson et. al. 2012). Similar results for the *eb1b-2* allele in Col-0 are not available.

Root responses to mechanical cues of *eb1b-1* and mutants with defects in auxin transport were compared by analyzing seedlings growing on the surface of agar plates reclined from a vertical orientation (Fig. 1). Under these conditions, gravitropism presses the root tip against the agar surface and this contact mechanically stimulates the root as it grows. On plates reclined 20º from vertical, roots of the wild type Arabidopsis accessions Ws and Col-0 both exhibited a waving pattern of growth that was slightly skewed towards one side of the plate and they rarely formed loops (Fig. 1). In contrast to wild type, roots of *eb1b-1* mutants skewed more towards the left when viewed from above the agar surface and they formed more loops than wild type Ws. Approximately

16% of *eb1b-1* roots formed loops, a proportion that was significantly greater than the proportion of loops formed by Ws roots (2%, P = 0.0008). As observed for *eb1b-1* mutants, seedlings carrying mutations in *AUX1* and *PIN2* genes had roots that formed more loops than wild type; 49% of *aux1-7* and 60% of *eir1-1* roots formed loops, proportions that were significantly greater than wild type Col-0 roots (0%, P < 0.001). These observations indicate that both auxin transport and EB1b have inhibitory effects on loop formation in roots responding to mechanical cues.

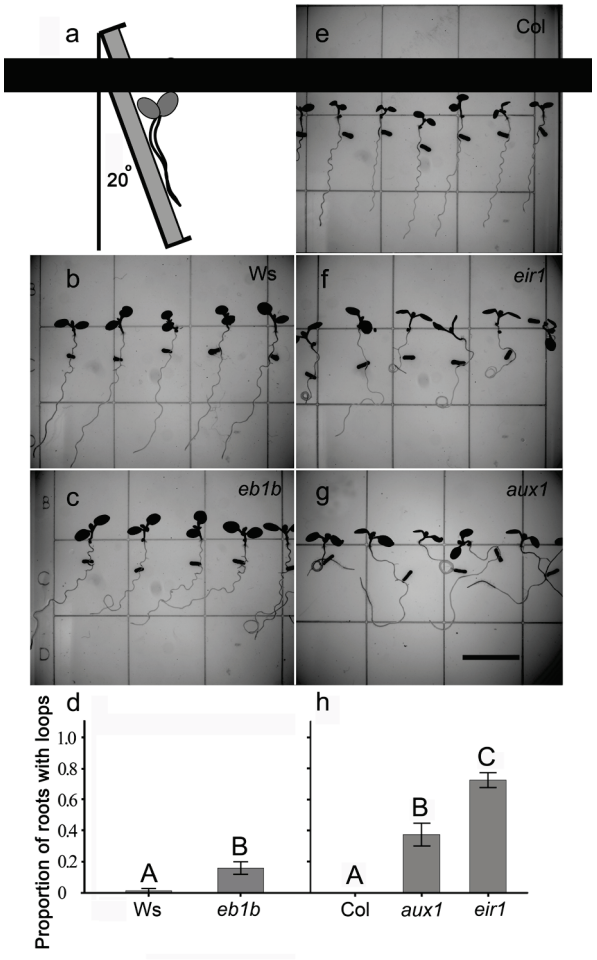

Figure 2.1. Both eb1b-1 and auxin transport mutants have roots that form more loops than wild type plants when grown on reclined agar plates.

Ws (b), eb1b-1 (c), as well as Col-0 (e), eir1-1 (f), and aux1-7 (g) seedlings were germinated on plates reclined 20° from the vertical (a) and the proportions of roots that formed loops were determined after 7 d (d, h). Data represents averages (grey bars) from 3-10 experiments (n for each genotype ranged from 58-195 seedlings). Error bars represent 1 standard error (SE). A, B, and C refer to statistically different averages (P<0.0001; Tukey's test). Size bar in (g) represents 1cm and applies to all photographs.

To determine whether EB1b function might be linked to auxin transport, loop formation was assessed in seedlings growing on reclined agar plates supplemented with different chemicals that disrupt auxin homeostasis. Treatments included the auxin transport inhibitors NPA and TIBA, an auxin signaling inhibitor PCIB, as well as the endogenous auxin IAA and two auxin analogs NAA and 2, 4-D. For comparative purposes, loop formation in *aux1-7*, *eir1-1,* and *eb1b-1 eir1-1* double mutant roots was also characterized.

2.3.1. eb1b-1 Roots are Hypersensitive to Reductions in Auxin Transport

NPA and TIBA, two chemical agents whose effects have been well-characterized in plants, were used to assess the effects of reducing auxin transport on root growth. Both chemicals inhibit auxin efflux and result in the accumulation of auxin inside cells (De Rybel et al. 2009). On agar plates reclined by 20º, both Ws and *eb1b-1* seedlings responded to increasing concentrations (up to 1 µM) of NPA by forming more loops (Fig. 2). At low concentrations of NPA (0.1 µM), both *eb1b-1* and Ws roots formed more loops than they did on plates without the inhibitor and the amount of looping increased to a maximum in seedlings grown on 1 µM NPA. Although NPA induced loop formation in both *eb1b-1* and Ws, the increase observed in *eb1b-1* mutants was significantly greater than that of Ws, indicating that reductions in auxin transport enhance root responses to mechanical cues to a greater extent in *eb1b-1* mutants than in wild type. Between 0.1 and 1 µM NPA, the proportion of roots with loops increased by 58% in *eb1b-1* and by only 34% in Ws ($P = 0.004$). Root elongation was only slightly reduced at 1 µM NPA, and concentrations higher than 0.1 µM inhibited root elongation to the same extent in mutant and wild type roots, indicating that the increase in looping is due to reductions in auxin transport and not a general response to perturbations in root growth (Fig. 2c). In contrast to *eb1b-1*, loop formation did not increase in *aux1-7* and *eir1-1* mutants exposed to NPA. When *aux1-7* seedlings were grown on plates containing NPA, the proportion of roots that formed loops was equivalent to that of solvent only controls and in *eir1-1* the amount of looping decreased when 1 µM NPA was added to the agar (Fig. 2b). At these concentrations of NPA, root elongation was largely unaffected in Col-0, *aux1-7,* and *eir1-1* (Fig. 2d), suggesting that the effect on looping is not due to a general perturbation in root growth.

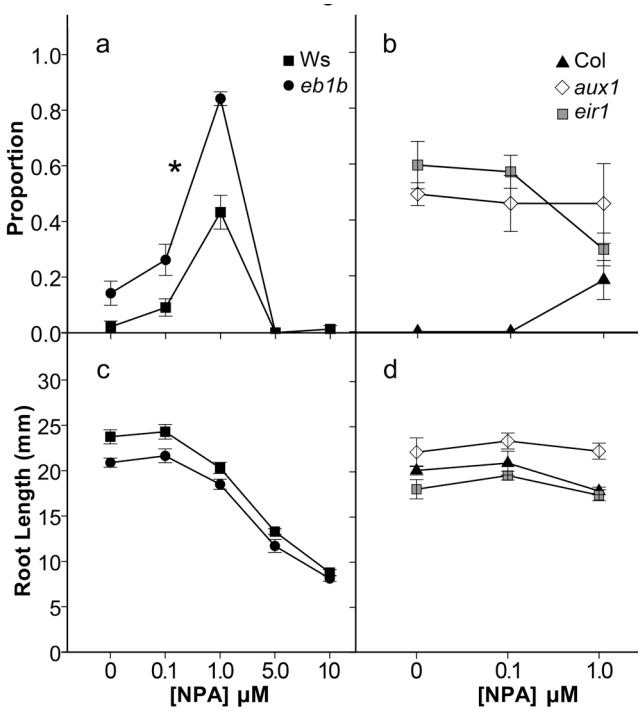

Figure 2.2. Roots of eb1b-1 mutants are hypersensitive to the auxin transport inhibitor NPA.

Ws, eb1b-1 (a, c) as well as Col-0, eir1-1, and aux1-7 (b, d) seedlings were grown on plates reclined 20° from vertical with or without NPA for 7 d at which time the proportions of roots that formed loops (a, b) and root lengths (c, d) were determined. Data points represent averages from 3-8 experiments (n = 51-151 seedlings). Error bars represent 1 SE. Asterisk denotes a statistical difference in response between eb1b-1 and Ws roots ($P < 0.01$; 2 factor ANOVA).

The second auxin transport inhibitor, TIBA, had effects on loop formation that were similar to those of NPA in all of the genotypes tested. TIBA induced loops in both *eb1b-1* and Ws roots, although *eb1b-1* responded at a lower concentration of TIBA than did Ws (Fig. 3a). The proportion of *eb1b-1* roots with loops increased from 14% to 29% between 0 and 0.1 µM TIBA, while loop formation in Ws did not increase until the concentration of TIBA reached 1 µM. The increase observed in *eb1b-1* was significantly greater than that of Ws ($P=0.0346$). The fact that *eb1b-1* responded to lower concentrations of TIBA than Ws indicates that, as observed for NPA, *eb1b-1* mutants were hypersensitive to TIBA. The effects of TIBA on loop formation in *aux1-7* and *eir1-1* roots also mimicked those of NPA. Growth of *aux1-7* seedlings on plates containing TIBA did not alter the proportions of roots that formed loops even at concentrations as

high as 10 μM, indicating that these seedlings were resistant to the effects of the inhibitor (Fig. 3b). As was observed on NPA, *eir1-1* responded to higher concentrations of TIBA by reducing loop formation at concentrations above 1 μM. The effects of TIBA on root elongation also resembled those of NPA. On increasing concentrations of TIBA, root elongation in both *eb1b-1* and Ws was inhibited in a similar dose dependent manner. Root elongation was also reduced in Col-0 roots at concentrations above 0.1 μM, while *aux1-7* and *eir1-1* exhibited slight reductions in root length only at the highest concentration of TIBA (10 μM). Taken together, these results indicate that *eb1b-1* roots are hypersensitive to the effects of auxin transport inhibitors while *aux1-7* and *eir1-1* roots are more resistant.

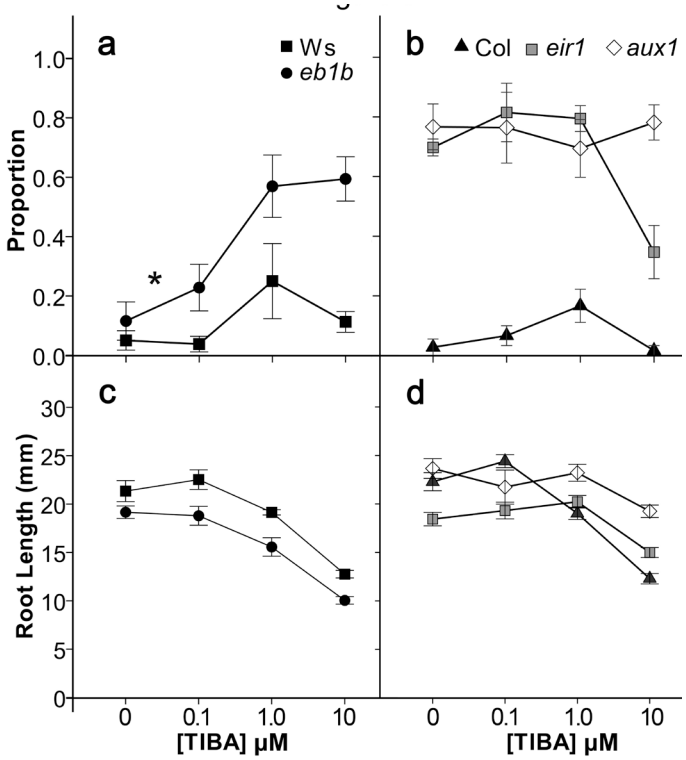

Figure 2.3. Roots of eb1b-1 mutants are more sensitive than wild type to TIBA.

Ws, eb1b-1 (a, c) as well as Col-0, eir1-1, and aux1-7 (b, d) seedlings were grown on plates reclined 20° from the vertical with or without TIBA for 7 d at which time the proportions of roots that formed loops (a, b) and root lengths (c, d) were determined. Data points represent averages from 3-6 experiments (n = 60-124 seedlings) and error bars denote 1 SE. A statistical difference in response between eb1b-1 and Ws roots is indicated by an asterisk ($P < 0.01$; two factor ANOVA).

The effects of disrupting auxin transport in *eb1b-1* mutants were also assessed by analyzing root growth in *eb1b-1 eir1-1* double mutants. When seedlings were grown on agar plates reclined by 20º, double mutants made more loops (71%) than did *eir1-1* single mutants (56%). The fact that the double mutants made more loops than *eir1-1* single mutants is consistent with the results obtained when auxin transport was reduced by chemical treatments and supports a model in which EB1b and PIN2 affect looping differently.

2.3.2. NPA Reduces Auxin Transport by Equivalent Amounts in eb1b-1 and Wild Type Roots

To determine whether the hypersensitivity of *eb1b-1* mutants to auxin transport inhibitors might be correlated with equivalent changes in auxin transport, a GFP-based auxin response biosensor was used to assess the effects of NPA on auxin transport in *eb1b-1* roots. Wild type and *eb1b-1* seedlings expressing the *DR5rev::GFP* construct (Benková et al. 2003; Friml et al. 2003) were grown on reclined agar plates that contained 0, 0.1, or 1 µM NPA and the relative amount of auxin transported basipetally, from the root cap towards the elongation zone, was estimated by measuring changes in GFP fluorescence in epidermal cells located behind the meristem (Fig. 4). To account for differences in basal levels of GFP fluorescence between roots, ratios of epidermal cell to cortical cell pixel intensities were calculated for each root. As expected, a dose-dependent decrease in GFP fluorescence was observed in epidermal cells of wild type roots treated with increasing concentrations of NPA, reflecting decreases in basipetal auxin transport associated with increasing concentrations of NPA. This result is consistent with the known effects of NPA on basipetal auxin transport in roots (Rashotte et al. 2000). Furthermore, the assay did not detect any differences in auxin transport between *eb1b-1* and wild type roots. Of particular relevance is the fact that the decreases in auxin transport between 0.1 and 1 µM NPA observed in *eb1b-1* mutants and wild type plants were indistinguishable, as this is the concentration range at which *eb1b-1* exhibited hypersensitivity with respect to loop formation. This analysis indicates that NPA had similar effects on auxin transport in both *eb1b-1* mutants and wild type roots and suggests that the additional looping seen in *eb1b-1* mutants is not correlated with larger changes in auxin transport.

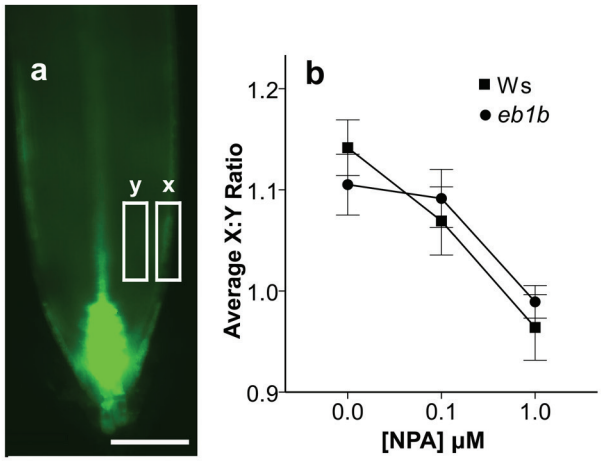

Figure 2.4. NPA affects auxin transport equivalently in eb1b-1 and Ws roots.

Seedlings expressing the DR5rev::GFP construct were grown on plates reclined 20° from vertical with or without NPA for 7 d at which time GFP in the root tip was visualized by epifluorescence microscopy. A representative image of a Ws root grown without NPA is shown (a). Pixel intensities were measured in epidermal and cortical cells located behind the meristem (white boxes shown in a, labeled x and y respectively) and average x:y ratios were calculated for each root. A plot of the average x:y ratios of eb1b-1 and Ws roots with and without NPA (b) revealed that both auxin transport and the effects of NPA on auxin transport were equivalent in the two genotypes. Size bar in (a) represents 100 µm Data points represent averages from 3 experiments (n = 23-27 seedlings) and black bars represent 1 SE.

2.3.3. Auxin Signaling Modulates Loop Formation in Roots

Since *eb1b-1* mutants did not appear to have defects in transporting auxin from the root cap to the elongation zone, we assessed the possibility that EB1b proteins could be affecting processes that occurred after auxin perception. Root responses to mechanical cues were analyzed in seedlings grown in the presence of PCIB, thought to be an inhibitor of auxin signaling events. This chemical reduces auxin-induced regulation of gene transcription by the TRANSPORT-INHIBITOR RESISTANT1 (TIR1) receptor (Oono et al. 2003). We found that the addition of 0.5 µM PCIB to the agar media enhanced loop formation in both Ws and *eb1b-1* roots, suggesting that TIR1-mediated signaling had an inhibitory effect on root responses to mechanical cues (Fig. 5). However, in contrast to Ws, roots of *eb1b-1* mutants exhibited a larger increase in loop formation and this increase was sustained at 1 µM PCIB, a concentration that reduced looping in Ws roots (Fig. 5a). At 1 µM PCIB, *eb1b-1* roots formed significantly more loops than did Ws ($P<0.0001$). The increase in loop formation in *eb1b-1* roots in the

presence of PCIB indicates that EB1b proteins enhance an inhibitory effect of TIR1 signaling on root responses to mechanical cues. PCIB also reduced root elongation, but significant decreases in elongation were detected only at concentrations of PCIB above those that affected loop formation (Fig. 5b). In contrast to loop formation, PCIB had similar effects on root elongation in *eb1b-1* mutants and Ws, indicating that the effects of TIR1 signaling on root elongation is not altered in *eb1b-1* mutants.

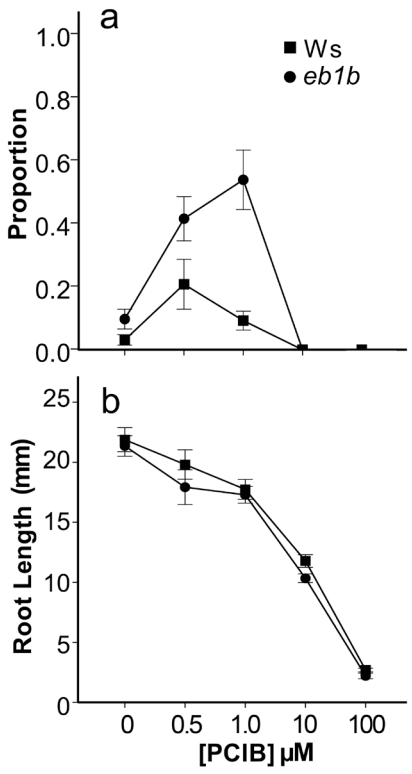

Figure 2.5. Roots of eb1b-1 mutants exhibit an enhanced and sustained sensitivity to PCIB.

Seedlings were grown on plates reclined 20° from the vertical with or without PCIB for 7 d and the proportions of roots that formed loops (a) and root lengths (b) were determined. Data points represent averages from 3-4 experiments (n = 17-113 seedlings) Error bars represent 1 SE.

2.3.4. Effects of IAA, NAA and 2, 4-D on Root Responses to Mechanical Cues

Since EB1b appears to affect processes mediated by auxin perception, we assessed the effects of increased auxin levels on root responses to mechanical cues.

The endogenous auxin IAA as well as two synthetic analogs, NAA and 2, 4-D were used in these experiments. To enable detection of either increases or decreases in the response, roots were grown on plates reclined to 45º from the vertical position. This growth regime provides relatively high levels of mechanical stimulation and causes roots to form more loops than they do when grown on plates reclined by 20º (Gleeson et al. 2012). We found that IAA and NAA had similar, mild effects on root responses to mechanical cues. 2, 4-D, on the other hand, had very different effects from those of IAA and NAA. IAA had small effects on looping in *eb1b-1* and Ws. In *eb1b-1* roots there was a slight increase in loop formation when the concentration of IAA was increased from 0 to 10 nM.

When *eb1b-1* and Ws seedlings were treated with 5 or 10 nM IAA the proportion of roots with loops did not change significantly when compared with untreated controls, although there was a slight increase at 5 nM for both genotypes (Fig. 6a). At 10 nM IAA there was a small increase in the proportion of roots with loops in *eb1b-1* and a small decrease in Ws. Looping decreased a little more in both genotypes between 10 and 17.5 nM IAA, although for both genotypes the proportions of loops formed in 17 nM IAA was not significantly different from untreated controls. In the *aux1-7* and *eir1-1* mutants, IAA increased looping to high levels at all concentrations tested, but had little effect on Col-0 wild type (Fig. 6b). As expected, IAA reduced root elongation in *eb1b-1*, Ws, and Col-0 roots but had little effect on root elongation in the auxin transport mutants (Fig. 6c, d).As observed for IAA, NAA also had minimal effects on looping in *eb1b-1* and Ws seedlings (Fig. 7a). Relatively small increases in loop formation were observed for both genotypes. Slight increases in loop formation in response to NAA were also observed in Col-0, and the auxin transport mutants (Fig. 7b). At 0.1 μM NAA, *eb1b-1* roots made significantly more loops than Ws ($P<0.0001$). As expected, NAA also decreased root elongation at concentrations above 0.01 μM (Fig. 7c, d). In contrast to IAA and NAA, 2, 4-D reduced loop formation in all of the genotypes tested, although *aux1-7* roots were somewhat resistant to the effects of 2, 4-D (Fig. 8a, b). Reductions in root elongation were also observed at higher concentrations of 2, 4-D with *aux1-7* roots again exhibiting a greater degree of resistance (Fig. 8c, d).

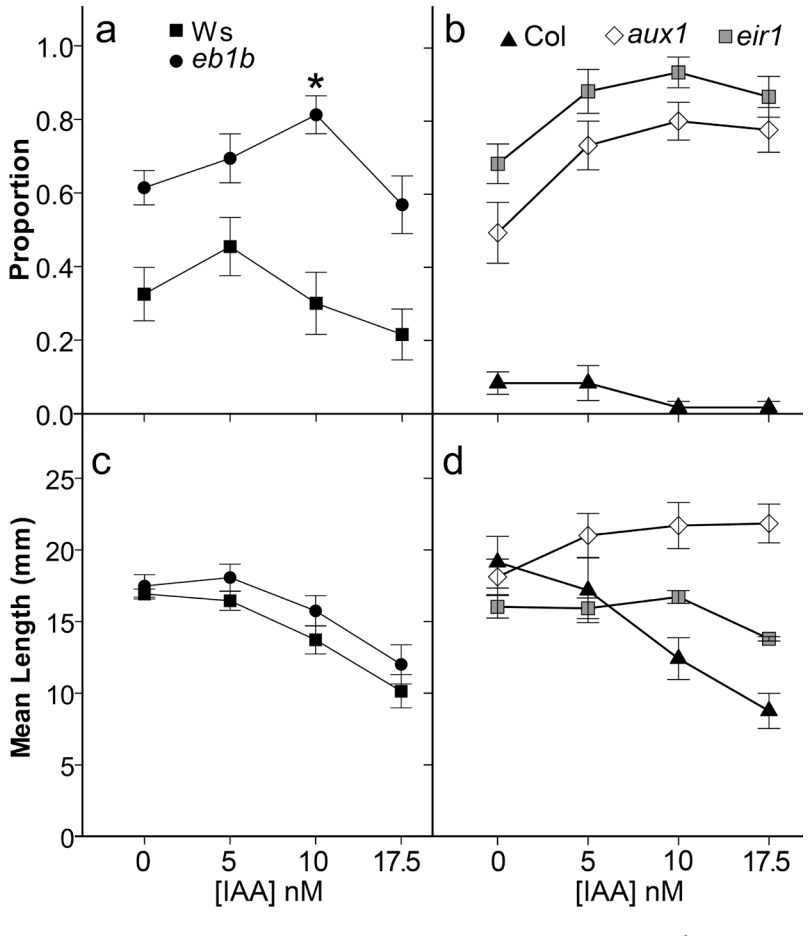

Figure 2.6. Effects of IAA on root responses to mechanical cues.

Ws, eb1b-1 (a, c), as well as Col-0, eir1-1, and aux1-7 (b, d) seedlings were transferred to plates with or without IAA three days after germination and grown for an additional four days reclined 45º from vertical. Data points represent averages from 3-4 experiments (n = 58-80 seedlings).

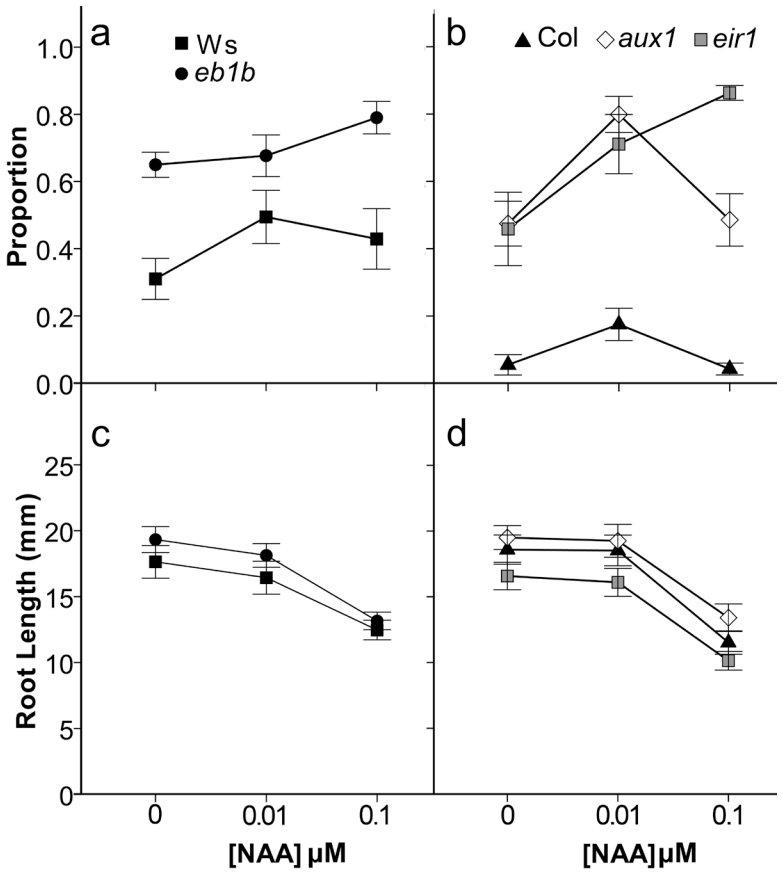

Figure 2.7. Effects of NAA on root responses to mechanical cues.

Ws, eb1b-1 (a, c), as well as Col-0, eir1-1, and aux1-7 (b, d) seedlings were transferred to plates with or without NAA three days after germination and grown for an additional four days reclined 45º from vertical. Data points represent averages from 5 experiments (n = 89-100 seedlings).

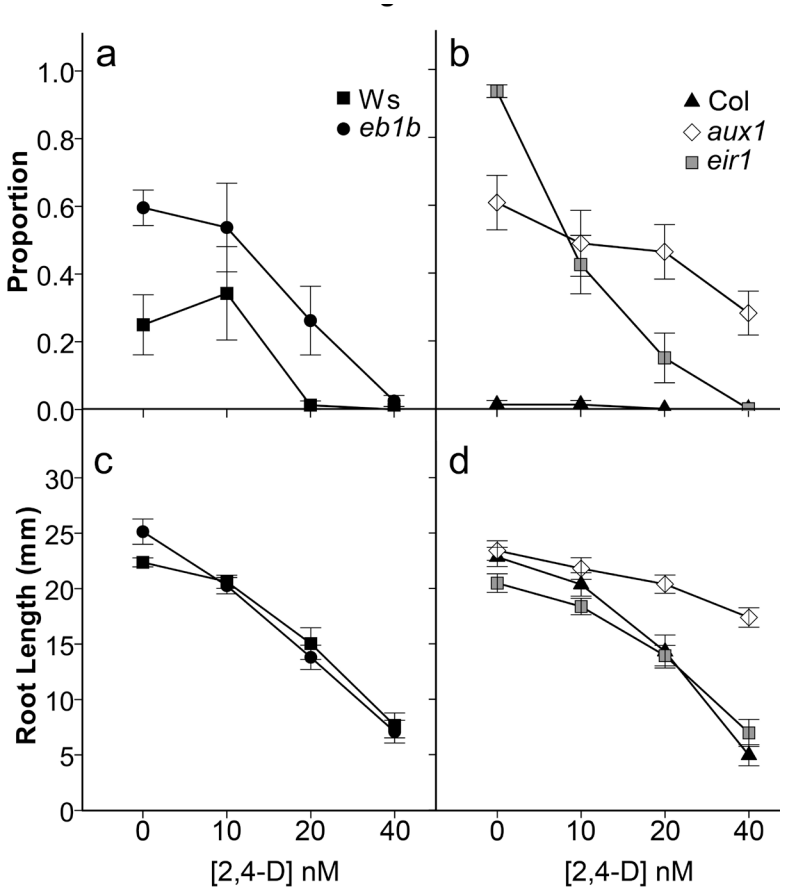

Figure 2.8. 2, 4-D reduces root responses to mechanical cues.

Ws, eb1b-1 (a, c), as well as Col-0, eir1-1, and aux1-7 (b, d) seedlings were transferred to plates with or without 2, 4-D three days after germination and grown for an additional four days reclined 45º from vertical. Data points represent averages from 4 experiments (n = 59-80 seedlings). Error bars represent 1 SE.

2.4. Discussion

Here we investigate the relationship between the microtubule associated protein EB1b and auxin in roots responding to mechanical cues. Both *eb1b-1* and mutants with defects in auxin transport exhibit greater responses to mechanical cues than wild type plants, indicating that auxin transport and EB1b both have repressive effects on the response in wild type plants. To assess the possibility of a functional link, we examined the effects of auxin transport inhibitors on root responses to mechanical cues. For comparative purposes, both *eb1b-1* and mutants with defects in auxin transport were examined. We found that root responses to mechanical cues did not increase when

seedlings carrying mutations in the AUX1 and PIN2 influx/efflux carriers were treated. This result is consistent with an inability of the inhibitor to further disrupt a process that is already defective in these mutants. In contrast, *eb1b* mutants exhibited significantly greater responses to mechanical cues in the presence of auxin transport inhibitors than did wild type plants (see Figs. 2, 3). The ability of the inhibitors to elicit greater responses in *eb1b-1* mutants suggests that EB1b and the inhibitors affect root responses to mechanical cues differently. In a scenario where EB1b and the inhibitors both act in the same way, *eb1b* mutants are expected to be either more resistant to the effects of the inhibitor or to, at most, increase loop formation by the same amount as seen in wild type plants. Instead, auxin transport inhibitors significantly enhanced the responses of *eb1b* roots to mechanical cues. Further evidence supporting the contention that EB1b and auxin transport modulate root looping differently was obtained through the analysis of *eb1b-1 eir1-1* double mutants. We found that *eb1b-1 eir1-1* double mutants made more loops than *eir1-1,* indicating that EB1b and PIN2 proteins repress loop formation by different mechanisms. Finally, we also analyzed auxin transport in seedlings expressing the auxin response biosensor *DR5rev::GFP*. Both *eb1b-1* and wild type roots treated with the auxin transport inhibitor NPA exhibited dose-dependent reductions in basipetal auxin transport that were indistinguishable from wild type roots at the same NPA concentrations that caused excessive looping in *eb1b-1* mutants. Taken together these results suggest that EB1b does not repress root responses to mechanical cues by altering the amount of auxin transported from the root cap to the elongation zone.

We also found that PCIB, a repressor of auxin-induced gene expression (Oono et al. 2003), enhanced loop formation in *eb1b-1* roots to a much greater extent than it did in wild type. As discussed above for the auxin transport inhibitors, the fact that PCIB induced a greater response in mutants than wild type suggests that EB1b and PCIB also affect root responses to mechanical cues in different ways. PCIB is thought to impair auxin signaling by acting as a competitor of auxin-induced regulation of gene transcription by the TIR1 receptor (Oono et al. 2003). Our result, therefore, suggests that EB1b does not affect TIR1. Thus, the possibility that EB1b represses root responses to mechanical cues specifically through a TIR1-mediated auxin signaling pathway seems

unlikely. However, we cannot rule out a role for EB1b on a signaling pathway mediated by PCIB-insensitive auxin receptors.

In contrast to the auxin transport inhibitors and PCIB, 2, 4-D had strikingly different effects on root responses to mechanical cues, causing reductions in loop formation in *eb1b-1,* Ws, and *eir1-1* roots. This effect also differed from that of the other auxins, an observation that has been previously reported in the literature. For example, IAA and NAA were found to inhibit root elongation by reducing the length of the growth zone in the root, while 2, 4-D affected cell production rates and actin-dependent processes (Rahman et al. 2007). Although the mechanism by which 2, 4-D elicits unique responses in plants is unknown, it may involve a difference in its ability to bind and activate auxin receptors in cells. 2, 4-D is known to bind the TIR1 receptor with a lower affinity than IAA (Kepinski and Leyser 2005; Rahman et al. 2006).

Another difference between the three auxin analogs is the mechanisms by which they are transported into and out of cells and the degree to which each chemical concentrates inside cells. While the entry and exit of IAA depends on auxin influx and efflux carriers, NAA diffuses into cells passively and exits via an efflux carrier. 2, 4-D enters cells through the influx carriers but it is not able to use the efflux carrier which can cause it to accumulate to higher levels inside cells than the other auxins (Delbarre et al. 1996). Perhaps it is the accumulation of 2, 4-D inside cells of both the root cap and the elongation zone that causes the reductions in loop formation observed in wild type, *eb1b-1,* and *eir1-1* roots. It has been reported that 2, 4-D cannot be redistributed appropriately in roots and that it disrupts gravitropic responses (Ottenschlager et al. 2003). If this is the explanation for the reduced responses to mechanical cues in our assay, it is of interest to note that 2, 4-D has the same effect in wild type, *eb1b-1,* and *eir1-1* roots, implying that 2, 4-D is able to accumulate inside the cells and that the influx carriers are functioning normally in all three genotypes. In contrast, *aux1-7* mutants are resistant to 2,4-D, as would be expected for seedlings lacking functional influx carriers. In contrast to 2,4-D , normal auxin gradients form in roots treated with IAA and NAA (Ottenschlager et al. 2003). This observation could explain why we observed only small effects on looping in our assays. If PIN proteins are functioning normally in both Ws and *eb1b-1* roots treated with IAA or NAA*,* normal auxin gradients would form in the roots and this could result in relatively minor effects on looping. Our observations that

exogenously applied IAA or NAA did not have large effects on either *eb1b-1* or Ws roots suggests that *eb1b-1* does not have major impairments in auxin transport.

In summary, EB1b, auxin transport, and auxin signaling all repress root responses to mechanical cues (Bisgrove et al. 2008; Gleeson et al. 2012; this paper). However, the fact that *eb1b-1* mutants exhibit greater responses to mechanical cues when treated with inhibitors of auxin transport or signaling suggest that EB1b may act by a different mechanism. Alternatively, one of the results of auxin signaling may be on EB1b activity. For example, interactions between EB1b and its binding partners, either microtubules or other proteins, may be altered. This would, in turn, result in a repression of root responses to mechanical cues. EB1b is known to be a key regulatory component of the protein complexes that form on microtubule ends (Akhmanova and Steinmetz 2010).

2.5. References

Akhmanova A, Steinmetz MO (2010) Microtubule +TIPs at a glance. J Cell Sci 123:3415-3419.

Benková E, Michniewicz M, Sauer M, Teichmann T, Seifertová D, Jürgens G, Friml J (2003) Local, efflux-dependent auxin gradients as a common module for plant organ formation. Cell 115:591-602.

Bisgrove SR, Hable WE, Kropf DL (2004) +TIPs and microtubule regulation. The beginning of the plus end in plants. Plant Physiol 136:3855-3863.

Bisgrove SR, Lee Y-RJ, Liu B, Peters NT, Kropf DL (2008) The microtubule plus-end binding protein EB1 functions in root responses to touch and gravity signals in Arabidopsis. Plant Cell 20:396-410.

Chan J, Calder GM, Doonan JH, Lloyd CW (2003) EB1 reveals mobile microtubule nucleation sites in *Arabidopsis*. Nat Cell Biol 5:967-971.

Chehab EW, Wang Y, Braam J (2011) Mechanical force responses of plant cells and plants. In: Wojtaszek P (ed) Mechanical Integration of Plant Cells and Plants, vol 9. Signaling and Communication in Plants. Springer, Berlin Heidelberg, pp 173-194. doi:10.1007/978-3-642-19091-9_7

Chen R, Hilson P, Sedbrook JC, Rosen E, Caspar T, Masson PH (1998) The *Arabidopsis thaliana AGRAVITROPIC 1* gene encodes a component of the polar-auxin-transport efflux carrier. PNAS 95:15112-15117.

Clough SJ, Bent AF (1998) Floral dip: a simplified method for *Agrobacterium*-mediated transformation of *Arabidopsis thaliana*. Plant J 16:735-743.

Delbarre A, Muller P, Imhoff V, Guern J (1996) Comparison of mechanisms controlling uptake and accumulation of 2,4-dichlorophenoxy acetic acid, naphthalene-1-acetic acid, and indole-3-acetic acid in suspension-cultured tobacco cells. Planta 198:532-541.

De Rybel B, Audenaert D, Beeckman T, Kepinski S (2009) The past, present, and future of chemical biology in auxin research. ACS Chem Biol 4:987-998.

Dixit R, Chang E, Cyr R (2006) Establishment of polarity during organization of the acentrosomal plant cortical microtubule array. Mol Biol Cell 17:1298-1305.

Friml J (2010) Subcellular trafficking of PIN auxin efflux carriers in auxin transport. Eur. J. Cell Biol. 89:231-235.

Friml J, Vieten A, Sauer M, Weijers D, Schwarz H, Hamann T, Offringa R, Jurgens G (2003) Efflux-dependent auxin gradients establish the apical-basal axis of Arabidopsis. Nature 426:147-153.

Gleeson L, Squires S, Bisgrove SR (2012) The microtubule associated protein END BINDING 1 represses root responses to mechanical cues. Plant Sci 187:1-9.

Hashimoto T (2011) Microtubule and cell shape determination. In: Liu B (ed) Advances in Plant Biology, vol 1. The Plant Cytoskeleton. Springer, New York, pp 245-257

Honnappa S, Gouveia SM, Weisbrich A, Damberger FF, Bhavesh NS, Jawhari H, Grigoriev I, van Rijssel FJA, Buey RM, Lawera A, Jelesarov I, Winkler FK, Wüthrich K, Akhmanova A, Steinmetz MO (2009) An EB1-binding motif acts as a microtubule tip localization signal. Cell 138:366-376.

Jones B and Ljung K (2012) Subterranean space exploration: the development of root system architecture. Curr. Op. Plant Biol. 15:97-102.

Kepinski S, Leyser O (2005) The Arabidopsis F-box protein TIR1 is an auxin receptor. Nature 435:446-451.

Komaki S, Abe T, Coutuer S, Inze D, Russinova E, Hashimoto T (2010) Nuclear-localized subtype of end-binding 1 protein regulates spindle organization in Arabidopsis. J Cell Sci 123.:451-459.

Liu M, Yang S, Wang Y, Zhu H, Yan S, Zhang W, Quan L, Bai J, Xu N (2009) EB1 acts as an oncogene via activating beta-catenin/TCF pathway to promote cellular growth and inhibit apoptosis. Mol Carcin 48:212-219.

Luschnig C, Gaxiola A, Grisafi P, Fink GR (1998) EIR1, a root-specific protein involved in auxin transport, is required for gravitropism in *Arabidopsis thaliana*. Genes Dev 12:2175-2187.

Mathur J, Mathur N, Kernebeck B, Srinivas BP, Hulskamp M (2003) A novel localization pattern for an EB1-like protein links microtubule dynamics to endomembrane organization. Curr Biol 13:1991-1997.

Migliaccio F, Fortunati A, Tassone P (2009) Arabidopsis root growth movements and their symmetry: Progress and problems arising from recent work. Plant Signal Behav 4:183-190.

Monshausen GB, Gilroy S (2009) Feeling green: mechanosensing in plants. Trends Cell Biol 19:228-235.

Muday GK and Rahman A (2008) Auxin transport and the integration of gravitropic growth. In: Gilroy S and Masson PH (eds) Plant Tropisms. Blackwell, Ames Iowa, pp 47-77.

Okada K, Shimura Y (1990) Reversible root tip rotation in Arabidopsis seedlings induced by obstacle-touching stimulus. Science 250:274-276.

Oliva M, Dunand C (2007) Waving and skewing: how gravity and the surface of growth media affect root development in Arabidopsis. New Phytol 176:37-43.

Oono Y, Ooura C, Rahman A, Aspuria ET, Hayashi K-i, Tanaka A, Uchimiya H (2003) p-Chlorophenoxyisobutyric acid impairs auxin response in Arabidopsis root. Plant Physiol 133:1135-1147.

Peer WA, Blakeslee JJ, Yang H, and Murphy AS (2011) Seven things we think we know about auxin transport. Mol. Plant 4:487-504.

Rahman A, Bannigan A, Sulaman W, Pechter P, Blancaflor EB, Baskin TI (2007) Auxin, actin and growth of the Arabidopsis thaliana primary root. Plant J 50:514-528.

Rahman A, Nakasone A, Chhun T, Ooura C, Biswas KK, Uchimiya H, Tsurumi S, Baskin TI, Tanaka A, Oono Y (2006) A small acidic protein 1 (SMAP1) mediates responses of the Arabidopsis root to the synthetic auxin 2,4-dichlorophenoxyacetic acid. Plant J 47:788-801.

Rutherford R, Masson PH (1996) *Arabidopsis thaliana sku* mutant seedlings show exaggerated surface-dependent alteration in root growth vector. Plant Physiol 111:987-998.

Sun L, Gao J, Dong X, Liu M, Li D, Shi X, Dong J-T, Lu X, Liu C, Zhou J (2008) EB1 promotes Aurora-B kinase activity through blocking its inactivation by protein phosphatase 2A. Proc Natl Acad Sci USA 105:7153-7158.

Swarup R, Kargul J, Marchant A, Zadik D, Rahman A, Mills R, Yemm A, May S, Williams L, Millner P, Tsurumi S, Moore I, Napier R, Kerr ID, Bennett MJ (2004) Structure-function analysis of the presumptive Arabidopsis auxin permease AUX1. Plant Cell 16:3069-3083.

Thompson MV, Holbrook NM (2004) Root-gel interactions and the root waving behavior of Arabidopsis. Plant Physiol 135:1822-1837.

Van Damme D, Bouget F-Y, Van Poucke K, Inze D, Geelen D (2004) Molecular dissection of plant cytokinesis and phragmoplast structure: a survey of GFP-tagged proteins. Plant J 40:386-398.

Vaughn LM, Baldwin KL, Jia G, Verdonk JC, Strohm AK, Masson PH (2011) The cytoskeleton and root growth behavior. In: Liu B (ed) Advances in Plant Biology, vol 1. The Plant Cytoskeleton. Springer, New York, pp 307-326

3. Repression of root responses to mechanical cues by EB1b: Examining the effects of overexpression and of GFP fusions to the C-terminal tail.

3.1. Introduction

The highly conserved microtubule associated protein END BINDING 1 (EB1) belongs to a group of proteins known as +TIPs because they preferentially accumulate on growing microtubule ends. While bound to microtubules, EB1 proteins can affect microtubule growth rates and they interact with a diverse array of additional proteins. EB1 interacting partners include other microtubule regulatory proteins, factors that affect actin-related functions, and proteins that are part of signaling pathways (Akhmanova, 2008). Although database searches of the Arabidopsis proteome reveal many proteins with a motif known to interact with EB1 in mammalian cells (Jiang et al 2012; Honnapa et al 2009; S. Squires, unpublished), there is a paucity of biochemical data regarding EB1 binding partners. In plants, analyses of mutant phenotypes are providing information regarding EB1 function. There are three EB1 genes encoded in the Arabidopsis genome, *EB1a, EB1b,* and *EB1c.* Plants carrying mutations in *EB1b* have greater responses to mechanical cues than wild type, indicating that the EB1b protein functions as a repressor of the response.

Here we find that the expression level of EB1b correlates with the degree to which roots respond to the mechanical cues imparted on them when they are grown down along the surface of an agar plate. Higher expression levels of *EB1b* transgenes in *eb1b-1* mutants results in a reduction of root responses to mechanical cues compared to wild type plants. Transgenic mutants that express *EB1b* at intermediate levels similar to wild type have roots with responses that are equivalent to wild type and significantly reduced compared to untransformed mutants. In addition, transgenic seedlings that

express *EB1b* at levels higher than wild type have roots that skew less, form fewer loops, and are more resistant to the effects of the auxin transport inhibitor NPA than seedlings expressing *EB1b* at wild type levels. On the other hand, mutants expressing *EB1b-GFP* fusions have roots that respond to mechanical cues in a manner equivalent to untransformed *eb1b-1* mutants, regardless of the expression level of the *EB1b-GFP* transgene indicating that the fusion proteins are not fully functional. The EB1b-GFP fusions are capable of binding to growing microtubule ends, indicating that microtubule binding by EB1b is not sufficient for normal repression of root responses to mechanical cues.

3.2. Methods and Materials

3.2.1. Plant material and culture conditions

Wild type Wassilewskija (Ws) seeds were obtained from The Arabidopsis Information Resource (TAIR; http://www.Arabidopsis.org/). The *eb1b-1* allele has been characterized previously (Bisgrove, Lee et al. 2008; Gleeson, Squires et al. 2012). Transgenic *eb1b-1* plants were generated as follows. A construct consisting of the *EB1b* promoter and cDNA sequences fused to DNA encoding *GFP (EB1b-GFP)* in the binary vector pCAMBIA1300 was kindly provided by R. Dixit (Dixit, Chang et al. 2006). *Eb1b* promoter and cDNA sequences lacking GFP *(EB1b)* were obtained as described previously (Gleeson, Squires et al. 2012). Briefly, the *EB1b-GFP* fusion described above was used as a template in PCR reactions with the following primers: 5'-GGGGACAAGTTTGTACAAAAAAGCAGGCTYYAAGCTTCTCCTCTTTTTCTTTGTTT-3' and 5'-GGGGACCACTTTGTACAAGAAAGCTGGGTYTTCTCCTTTACTCATGGCTCC-3'. PCR products were recombined into the GATEWAY pDONRTM vector (Invitrogen), verified by sequencing, and recombined into the binary vector pMDC99 (Curtis and Grossniklaus 2003). Transgenic *eb1b-1* mutant lines expressing either *EB1b-GFP* or *EB1b* were then generated via *Agrobacterium*-mediated transformation (Clough and Bent 1998). Independent homozygous lines expressing either *EB1b-GFP* or *EB1b* were isolated based on hygromycin resistance. T2 seedlings were tested for hygromycin resistance and T3 seeds were collected from the T2 lines that segregated 3 hygromycin

resistant to 1 sensitive. T3 lines that were 100% hygromycin resistant were chosen for further analysis.

Seeds were sterilized using the vapor phase method (Clough and Bent 1998) and placed on the surface of 0.8% (w/v) agar (Phytablend, Caisson laboratories Inc.) plates with half-strength Murashige and Skoog (MS; Sigma-Aldrich) supplemented with 0.05% (w/v) 2-(N-morpholino)ethanesulfonic acid (MES; Sigma-Aldrich) and 1% (w/v) sucrose, pH 5.8. Seeds were vernalized in the dark at 4°C for 3-7 days and then grown at 20°C under a 16-h-light/8-h-dark cycle for either 4 or 7 days. Sensitivities to N-1-naphthylphthalamic acid (NPA) were assessed by germinating seedlings on agar plates containing either 0.05% dimethyl sulfoxide (DMSO) for the control plates, or 1μM of NPA dissolved in DMSO.

3.2.2. Phenotypic analyses

Seedlings were photographed with a Retiga 4000R digital camera mounted on an Olympus SZX16 stereo microscope and root phenotypes were assessed from photographs using either Photoshop or ImageJ software (http://rsbweb.nih.gov/ij/index.html). Statistical analyses were performed in JMP 7. Movies of EB1b-GFP comets were obtained with an inverted Zeiss epifluorescent microscope and Hamamatsu 1394 ORCA-ERA camera. Microtubule growth rates were calculated based on movement of the EB1b comets. Individual EB1b foci were tracked over 10 second intervals and the velocity was determined by computing the microns traveled over the time interval.

3.2.3. Extraction of nucleic acids and quantification of relative EB1b expression levels

For each genotype, RNA was extracted from three biological replicates of 4-day old seedlings (8 - 14 seedlings per replicate) using the RNeasy® kit (Qiagen). RNA was reverse transcribed using RevertAid™ H Minus First Strand cDNA Synthesis kit (Fermentas) according to the manufacturer's instructions using the oligo (dT) primers provided in the kit. The expression level of *EB1b* was quantified relative to that of a reference gene, *adenine phosphoribosyltransferase 1 APT1* (Gutierrez, Mauriat et al. 2008) from the cDNA samples using the DyNAmo™ Flash SYBR® Green qPCR Kit

(Thermo Scientific, Finnzymes), an Opticon™2 Real Time Detection System (Bio-Rad), and the following primers: *EB1b* forward 5'-GCATTATGAACGAGAAT-3', *EB1b* reverse 5'-ACTTCGGCTGATGAGTTGCT-3', *APT1* forward 5'-ACCGTTCAACCACCTCACTC-3', and *APT1* reverse 5'-AAAGGCCTCAGTGTCGAGAA-3'. qPCR reactions were optimized by performing a series of PCR amplifications using several annealing temperatures between 55 and 65 degrees and a series of 10-fold dilutions of a Ws cDNA template for each primer pair. At each annealing temperature, crossing threshold (CT) values, defined as the PCR cycle number at which the fluorescent signal became detectable above background levels, were plotted against the dilution factor and the slope of the line was used to calculate amplification efficiencies (E) by the following formula: $E = 10^{(-1/slope)}$. An annealing temperature of 65 degrees was chosen for use in the remaining PCR reactions since this temperature resulted in a near doubling of the PCR product with each amplification cycle (E values of 1.90 and 1.96 for the APT1 and EB1b primers respectively). Three technical replicates were carried out for each biological replicate. To ensure that the detected fluorescent signals represented either *EB1b* or *APT1* cDNAs, a melting curve analysis was performed on each PCR reaction, the amplified products were analyzed by agarose gel electrophoresis and they were sequenced. Relative *EB1b* expression levels were determined for each genotype by calculating the average CT values from the three technical replicates and using them in the following formula: $2^{(CT\ APT1 - CT\ EB1b)}$.

3.3. Results:

To determine whether altered levels of *EB1b* gene expression affect root responses to mechanical cues, we generated a series of transgenic *eb1b-1* mutant lines expressing either full-length EB1b *(EB1b)* or a fusion of the carboxy terminus of EB1b to GFP *(EB1b-GFP)*, both under the transcriptional control of the endogenous *EB1b* promoter (Dixit, Chang et al. 2006; Gleeson, Squires et al. 2012). Eight independent homozygous lines, 5 expressing *EB1b-GFP* fusions (EB1b-GFP L1 – L5) and 3 expressing *EB1b* alone (EB1b L1 - L3) were isolated as described in the Methods and Materials. *EB1b* expression levels, relative to an established reference gene, *APT1* (Gutierrez, Mauriat et al. 2008), were determined for wild type (Ws) seedlings and each

transgenic line via reverse transcription-quantitative real-time PCR (RT-qPCR; Fig. 1). EB1b-GFP L1, L3, L4, and L5 as well as EB1b L1 were all found to express *EB1b* at higher levels than the endogenous expression observed in wild type seedlings. Three lines had expression levels similar to that of wild type, EB1b-GFP L2, EB1b L2, and EB1b L3.

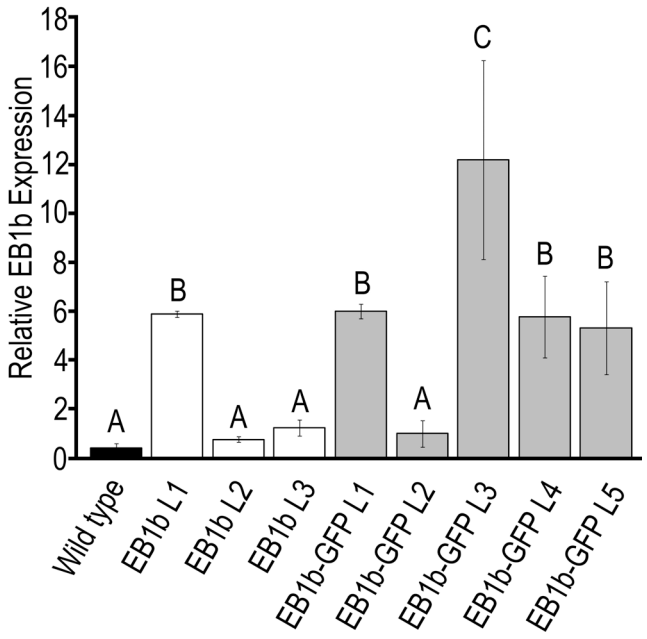

Figure 3.1. **EB1b *expression levels relative to* APT1 *in wild type and transgenic* eb1b-1 *lines.***

Bars represent averages of three biological replicates (18-42 seedlings) with standard deviations. The letters A, B and C indicate averages that are significantly different from one another (Students' T-test; $P < 0.05$).

3.3.1. Root growth analyses of wild type, eb1b-1 mutants, and transgenic lines

Responses of the transgenic lines, *eb1b-1* mutants, and wild type roots to mechanical cues were analyzed by growing seedlings on the surface of agar plates reclined away from a vertical position (Fig. 2). Roots growing down along the agar surface receive mechanical cues as they interact with the hard agar surface. When grown on plates reclined at shallow angles, 20° from vertical, both wild type and *eb1b-1* mutant roots skewed to one side instead of growing downwards (Fig. 2), although *eb1b-1* mutant roots skewed more than wild type. Root growth was also observed in seedlings

growing on agar plates reclined to 45°, a condition that provides additional mechanical cues to the root (Gleeson, Squires et al. 2012). Under these conditions both *eb1b-1* and wild type roots skewed more and several roots formed loops. Finally, root growth was analyzed in seedlings exposed to the auxin transport inhibitor NPA. This treatment reduces the ability of roots to respond to gravity and increases loop formation in roots growing on agar surfaces (Okada and Shimura 1990; Chen, Hilson et al. 1998; Vaughn, Baldwin et al. 2011). Consistent with previously reported analyses, NPA-treated *eb1b-1* roots appeared to form more loops than did NPA-treated wild type roots (Squires and Bisgrove 2013). Transgenic *eb1b-1* mutant lines expressing either *EB1b* or *EB1b-GFP* constructs exhibited a degree of root skewing that was equivalent to wild type, more vertical than wild type, or equivalent to *eb1b-1* mutants, depending on the nature of the transgene and its expression level (Fig. 2j-r). The two transgenic *eb1b* lines with *EB1b* expression levels similar to wild type (EB1b L2, L3) had roots that looked similar to wild type in all three assays. On the other hand, the overexpressing line (EB1b L1) appeared to grow straighter and to form fewer loops than wild type. Transgenic lines expressing *EB1b-GFP* fusions had roots that were more similar to *eb1b-1* mutants than they were to either wild type or the line that overexpressed *EB1b* (EB1b L1), regardless of the level of expression associated with the transgene.

Root responses to mechanical cues were quantified in three ways. 1) Root skewing angles were measured on seedlings grown on agar plates reclined 20° from vertical. 2) The proportions of roots that formed loops were determined for seedlings growing on agar plates reclined 45° from vertical. 3) The sensitivity of each genotype to the inhibition of auxin transport was assessed by determining the difference in the proportions of roots that formed loops in the presence and absence of NPA. In each of the three assays, *eb1b-1* mutant roots always exhibited higher skewing angles, formed more loops, and were more sensitive to NPA than wild type (Figs. 3, 4) consistent with previously published results (Bisgrove, Lee et al. 2008; Gleeson, Squires et al. 2012; Squires and Bisgrove 2013).

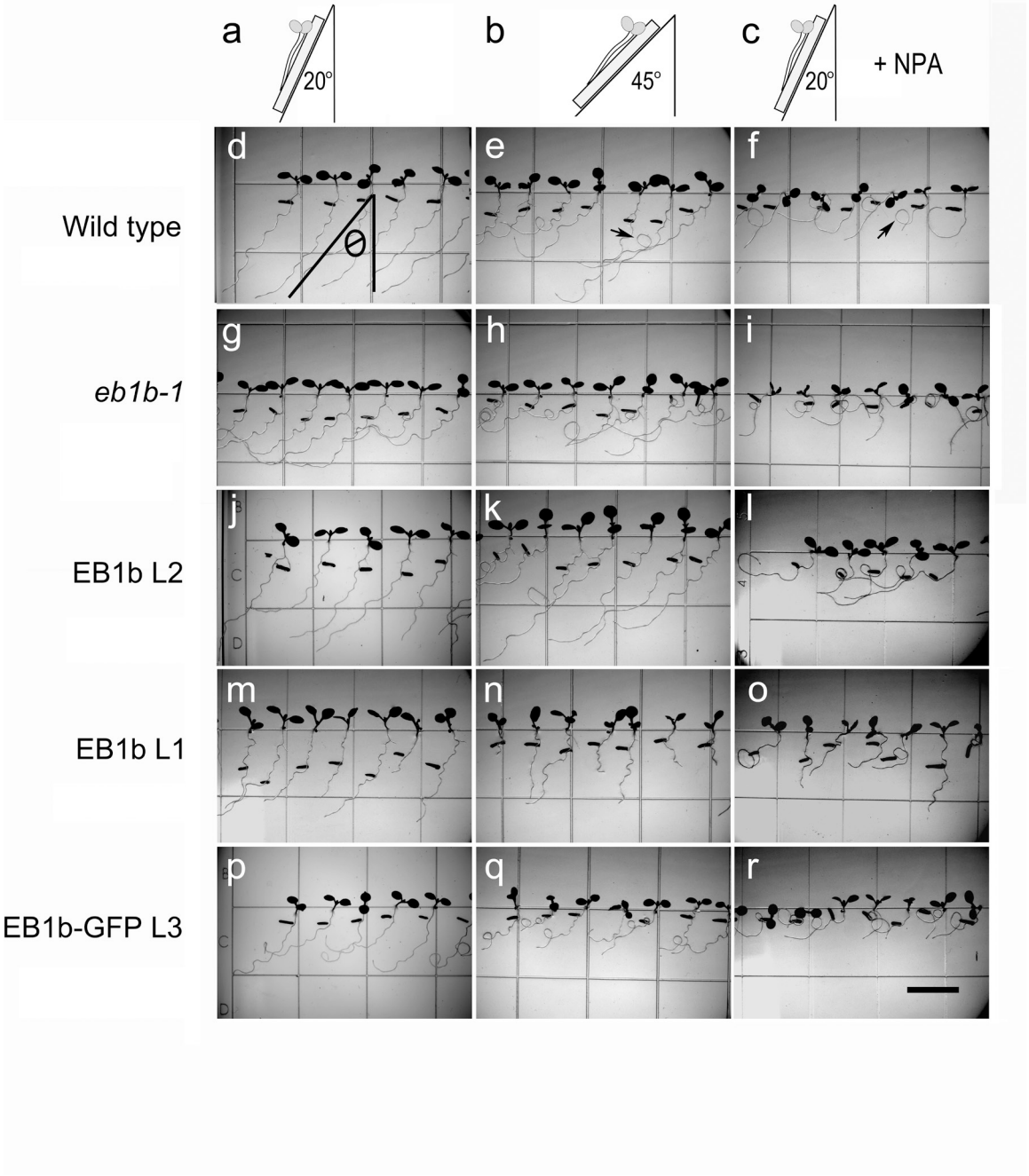

Figure 3.2. Phenotypes of roots responding to combinations of mechanical cues and gravity.

Root responses were assayed in three ways: on agar surfaces reclined at 20° (a,d,g,j,m,p), 45° (b,e,h,k,n,q), or 20° with 1μM NPA added to the agar (c,f,i,l,o,r). Root skewing angles, defined as the angle between the trajectory of root growth and a vertical line drawn parallel with the surface of the agar (d), and the amount of loops that formed (arrow, e) were observed in wild type (d-f), *eb1b-1* (g-i), EB1b L2 (j-l), EB1b L1 (m-o), and EB1b-GFP L3 (p-r). Size bar in r is 1 cm and applies to all photographs

3.3.2. *Root responses to mechanical cues are correlated with EB1b expression level*

Transgenic lines transformed with *EB1b* constructs exhibited responses that were reduced from those observed in untransformed *eb1b-1* mutants. When grown on plates reclined by 20° the roots of EB1b L1, L2, and L3 had average skewing angles that ranged from 24 - 35° (Fig. 3a). This level of skewing was significantly less than was observed for *eb1b-1* roots (44.7°; $P < 0.05$). As we previously reported (Gleeson, Squires et al. 2012), two transgenic lines, EB1b L2 and L3, had skewing angles that were equivalent to wild type (Fig. 3a). We now show that these lines correspond to transgenic mutants that also express *EB1b* at levels equivalent to wild type (Fig. 1). Roots of the overexpressing line, EB1b L1, skewed significantly less than both wild type and the transgenic lines that express *EB1b* at wild type levels ($P < 0.05$).

On plates reclined 45° from vertical, the proportions of roots that formed loops was significantly less in transgenic lines than it was in *eb1b-1* mutants (Fig. 3b). On average, less than 10% of roots of the overexpressing transgenic line, EB1b L1, formed loops, a proportion that was significantly lower than wild type (40%,< 0.05). Of the transgenic lines that express *EB1b* at levels equivalent to wild type, one line, Eb1b L2, had roots that looped to the same extent as wild type while the other line, Eb1b L3, made fewer loops. Similar reductions in loop formation were observed when transgenic seedlings were treated with NPA (Fig. 3c). NPA induced a greater increase in loop formation in *eb1b-1* mutant roots than it did in wild type and the increase in loop formation was significantly less in transgenic lines expressing *EB1b*. As was observed in the other two assays, overexpression of *EB1b* had the greatest effect, as the increase in loop formation induced by NPA was the lowest of all the genotypes tested including wild type in the overexpressing line EB1b L1. Taken together, these results suggest that EB1b has a repressive effect on root responses to mechanical cues and that the degree of repression is greater when *EB1b* is expressed at higher levels.

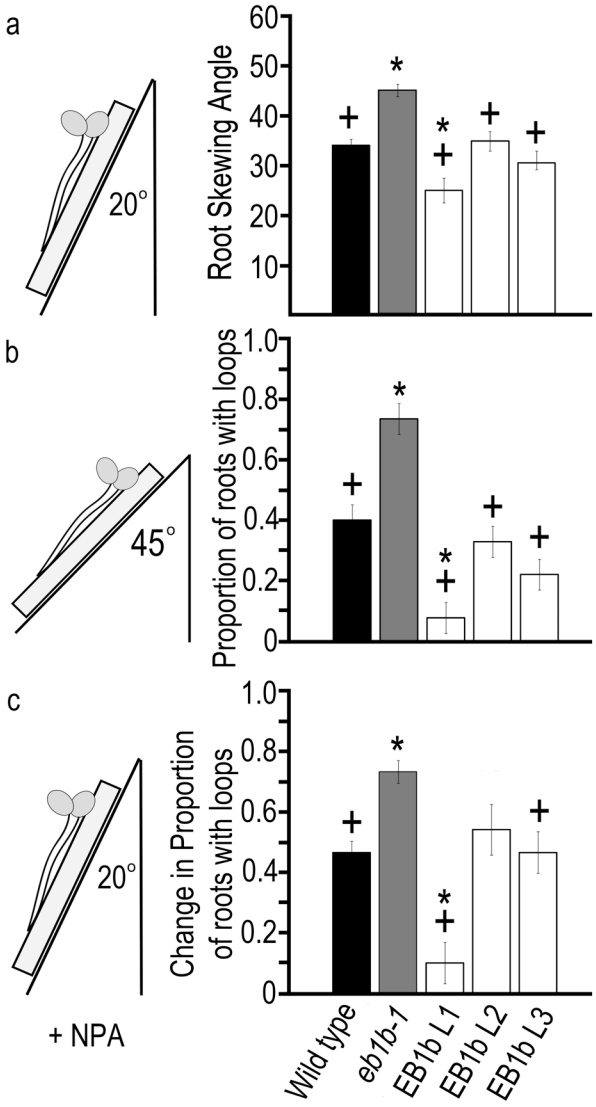

Figure 3.3. Quantification of root responses to touch/gravity stimulation in transgenic eb1b-1 mutants expressing EB1b constructs.

Skewing angles were measured on seedlings grown on agar plates reclined by 20^{o} (a). Proportions of roots that formed loops were determined for seedlings grown on plates reclined by 45^{o} (b). Sensitivities to NPA were assessed by determining the difference in the proportion of roots that made loops in the presence and absence of 1μM NPA for seedlings grown on plates reclined by 20^{o} (c). Averages with standard errors (SE) are reported. Averages that are significantly different (ANOVA, $P < 0.05$) from wild type or *eb1b-1* are denoted by symbols * and + respectively

3.3.3. EB1b-GFP fusions are functionally impaired

In contrast to the results obtained with *EB1b* transgenes, the expression of *EB1b-GFP* fusions in *eb1b-1* mutants had little to no effect on root responses to mechanical cues (Fig. 4). The average skewing angles of the EB1b-GFP lines ranged from 40 - 54°, values that were significantly greater than the angles measured for wild type roots (32.8°, $P < 0.01$) and similar to or greater than those of *eb1b-1* mutants (43.9°). The *EB1b-GFP* transgenes failed to reduce root skewing angles of *eb1b-1* mutants even in lines with relative expression levels that were 6 or 12 fold higher than wild type (EB1b-GFP L1 L3, L4, and L5). *EB1b-GFP* expression also failed to reduce looping in most transgenic *eb1b-1* roots tested on plates reclined 45° from vertical. In four of five transgenic lines, the average proportions of roots with loops ranged from 62-72%, amounts that were similar to *eb1b-1* mutants (73%) and significantly greater than wild type (40%; $P < 0.05$). In only one of the transgenic lines, EB1b-GFP L2, was the proportion of roots that formed loops reduced from the high levels seen in *eb1b-1* mutants to levels more similar to wild type. Finally, NPA induced increases in loop formation in *EB1b-GFP* transformants that were statistically similar to those measured for *eb1b-1*mutants, although in two lines the increase in loop formation was not as large as it was in the other three lines. EB1b-GFP L3 and EB1b-GFP L5, two of the four overexpressing lines, exhibited increases that fell halfway between the increases observed for *eb1b-1* and wild type. However, in none of our assays did we observe a reduction in looping or skewing that fell below the levels measured in wild type plants, even when the relative expression level of the *EB1b-GFP* fusion was close to 12 fold higher than *EB1b* expression in wild type. Thus, the ability of this transgene to repress root responses to mechanical cues appears to be compromised.

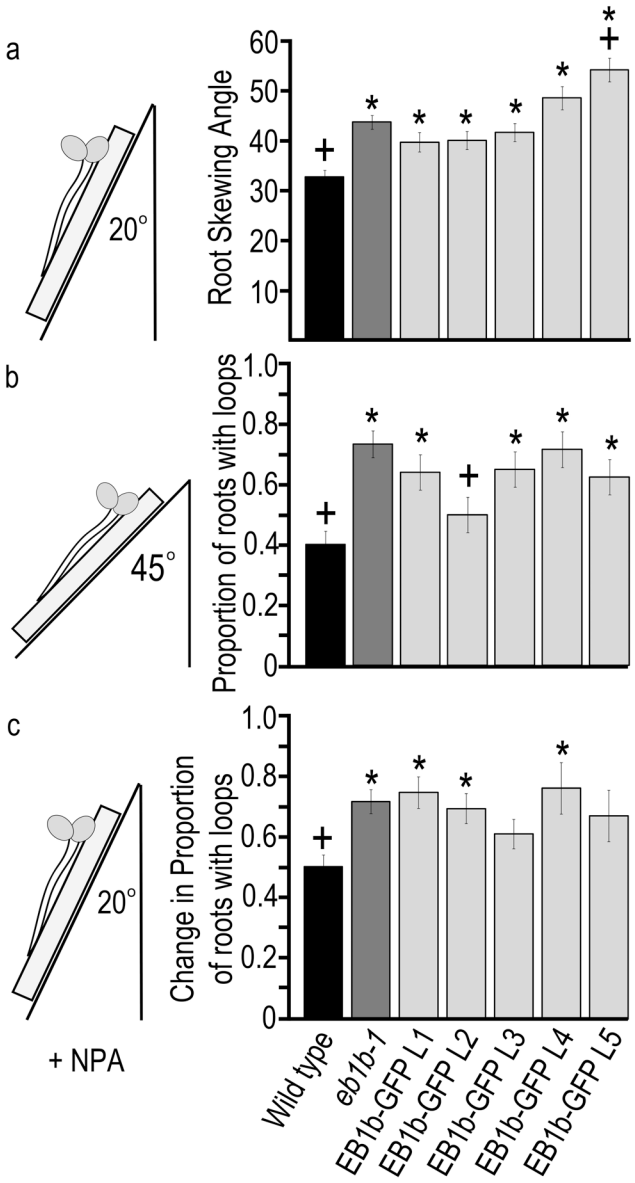

Figure 3.4. Quantification of root responses to touch/gravity stimulation in transgenic eb1b-1 mutants expressing EB1b-GFP constructs.

Root skewing angles (a), proportions of roots that formed loops (b), and sensitivities to NPA for each genotype are shown. Averages with standard errors (SE) are reported. Averages that are significantly different (ANOVA, $P<0.05$) from wild type or *eb1b-1* are denoted by symbols * and + respectively.

To determine whether the fusion of GFP to the carboxy terminus interfered with microtubule binding we examined root epidermal cells from the EB1b-GFP L3 and EB1b-GFP L2 lines which were shown to either overexpress the transgene or express it at

levels equivalent to wild type respectively. In both lines, EB1b-GFP fusions localized to the growing MT ends in the typical comet-shaped pattern previously reported in the literature indicating that they were able to bind MTs (Figure 5). To see whether overexpression of the EB1b-GFP construct affected MT growth rates we compared the velocities of the EB1b-GFP comets in the same two lines. We found that EB1b-GFP comets moved at similar velocities in both lines (6.5 ± 0.43 and 6.0 ± 0.98 μm/min, P = 0.41, Student's T-Test Table 1) suggesting that overexpression did not affect MT growth rates. A search of the literature for MT growth rates measured in a variety of plant cells revealed growth rates that ranged from 4.5 to 7.7 μm/min. We found three instances in which EB1b-GFP constructs are expressed reported in the literature. Two of these, p35S:EB1b-GFP, are likely to overexpress EB1b and the third, pEB1b:EB1b-GFP, is expected to be expressed at lower levels. In all three of these lines MT growth rates ranged from 4.5 to 6.8 μm/min. Our measurements for EB1b-GFP in root cells fall within these ranges. It is also worth noting that our measurements in roots are similar to the velocities observed in other cell types.

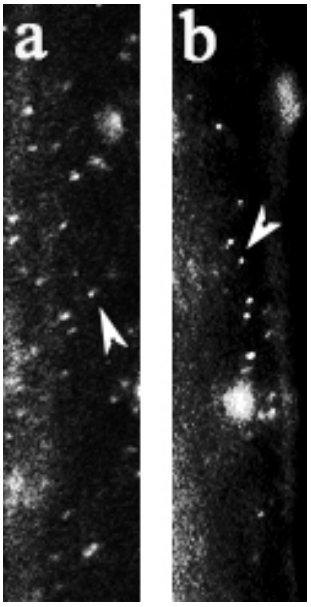

Figure 3.5. EB1b-GFP localizes to growing MT ends.

Epifluorescence images of portions of root epidermal cells show EB1b-GFP labeling the growing ends of MTs in characteristic comet shapes (arrows) in both EB1b-GFP L2 (a) and the over expressing line EB1b-GFP L3 (b).

Table 3.1. A comparison of microtubule growth rates

Cell type	Microtubule Label	Growth rate (μm/min)	Standard Deviation	Reference
Root	Eb1b-GFP L2	6.5	0.43	This report
	Eb1b-GFP L3	6.03	0.98	This report
Hypocotyl	p35S:EB1a-GFP	5.4	1.5	Crowell et al., 2011
	p35S:EB1a-GFP	5.2	1.5	Crowell et al., 2011
	p35S:EB1-GFP	6	0.5	Buschmann et al., 2009
	p35S:GFP-EB1b	4.54	1.64	Ishida et al., 2007
	GFP-TUB6	4.68	-	Ishida et al., 2007
	p35S:YFP-TUA5	7.4	4.9	DeBolt et al., 2007
	p35S:GFP-TUA6 (unbundled MTs)	7.33	2.49	Shaw and Lucas, 2011
	p35S:GFP-TUA6 (bundled MTs)	7.72	2.1	Shaw and Lucas, 2011
	p35S:GFP-TUA6	4.72	3.02	Abe and Hashimoto, 2005
	GFP-TUB6	5.13	2.71	Nakamura et al., 2004
	pMAP65-1:mCherry-MAP65-1	5.5	1.35	Lucas et al., 2011
BY-2 Cells	p35S:MBD-DsRed	5.6	1.92	Dixit and Cyr, 2004
	p35S:YFP-TUA6	6.15	3.05	Dixit and Cyr, 2004
	p35S:EB1b-GFP	6.8	0.89	Dhonukshe et al., 2005
	pEB1a:EB1a-GFP	5.1	0.7	Dixit et al., 2006
	pEB1b:EB1b-GFP	4.98	0.78	Dixit et al., 2006
***Arabidopsis* Cell Suspension**	p35S:EB1a-GFP	6.8	0.16	Chan et al., 2003

3.4. Discussion

Here we find that root responses to mechanical cues are correlated with expression levels of *EB1b*. Plants that do not express *EB1b* (*eb1b-1* mutants) had roots that formed loops and skewed strongly to the left, indicating an inability to repress responses to touch. At intermediate *EB1b* expression levels (EB1b-GFP L2), seedlings exhibited mild root growth phenotypes, similar in appearance to wild type roots. Plants that overexpressed *EB1b* grew straighter than wild type roots and had an enhanced ability to inhibit responses to touch. These observations support the idea that EB1b acts as a repressor of root responses to mechanical cues (Gleeson et al, 2012). The degree of repression is dependent on the expression level of *EB1b*.

In contrast, roots expressing *EB1b* with a GFP fusion at the C-terminus were unable to repress responses to touch. In each of the root growth assays, the phenotypes of the transgenic seedlings exhibited defects in root growth that were similar to *eb1b-1* mutants. The mutant phenotype was observed regardless of the expression level of the construct. Since plants expressing EB1b constructs without GFP inhibit root responses to touch, whereas EB1b-GFP fusions lack the repressive ability, it is possible that the C-terminal GFP tag interferes with the function of EB1b.

The cellular localization patterns of EB1b-GFP were examined in one transgenic line overexpressing the construct (EB1b-GFP L3), and in another that expressed EB1b-GFP at wild type levels (EB1b-GFP L2). In both lines, EB1b-GFP was able to bind to, and track the MT plus ends with velocities similar to those published by others. This result suggests that the root growth defects in these transgenic lines were not caused by defective EB1b-MT interactions. It has been previously reported that the addition of GFP to the C-terminus of EB1 interferes with its ability to interact with other, non-tubulin proteins (Skube 2009). The C-terminal domain of EB1 contains a domain involved in mediating protein-protein interactions (Jiang et al, 2012). We propose a model in which EB1b represses root responses to touch by interacting with other proteins via its C-terminal interaction domain. EB1b may concentrate or sequester proteins to the MT plus end where they may either activate or inhibit pathways involved in regulating responses to touch.

3.5. References

Abe T, Hashimoto T (2005) Altered microtubule dynamics by expression of modified alpha-tubulin protein causes right-handed helical growth in transgenic Arabidopsis plants. Plant J 43(2):191-204.

Akhmanova A, Steinmetz MO (2010) Microtubule +TIPs at a glance. J Cell Sci 123:3415-3419.

Bisgrove SR, Lee YRJ, Liu B Peters NT Kropf DL (2008) The microtubule plus-end binding protein EB1 functions in root responses to touch and gravity signals in Arabidopsis. Plant Cell 20(2): 396-410.

Buschmann H, Hauptmann M, Niessing D, Lloyd CW, and Schäffner AR (2009) Helical Growth of the Arabidopsis Mutant tortifolia2 Does Not Depend on Cell Division Patterns but Involves Handed Twisting of Isolated Cells. The Plant Cell 21(7):2090-2106.

Chan J, Calder GM, Doonan JH and Lloyd CW (2003) EB1 reveals mobile microtubule nucleation sites in Arabidopsis. Nature Cell Biology 5(11):967-971.

Chen R, Hilson P, Sedbrook J, Caspar T, Masson PH (1998) The *Arabidopsis thaliana AGRAVITROPIC 1* gene encodes a component of the polar-auxin-transport efflux carrier. Proc Natl Acad Sci U S A 95(25):15112-15117.

Clough SJ and AF Bent (1998) Floral dip: a simplified method for *Agrobacterium*-mediated transformation of *Arabidopsis thaliana*. Plant J 16(6): 735-743.

Crowell EF, Timpanoa H, Despreza T, Franssen-Verheijen T, Emons A, Höfte H and Vernhettes S (2011) Differential Regulation of Cellulose Orientation at the Inner and Outer Face of Epidermal Cells in the Arabidopsis Hypocotyl. The Plant Cell 23(7):2592-2605.

Curtis MD and Grossniklaus U (2003) A Gateway cloning vector set for high-throughput functional analysis of genes in planta. Plant Physiol 133: 462-469.

DeBolt S, Gutierrez R, Ehrhardt DW, Melo CV, Ross L, Cutler SR, Somerville C, and Bonetta D (2007) Morlin, an inhibitor of cortical microtubule dynamics and cellulose synthase movement. Proc Natl Acad Sci U S A. 104(14):5854–5859.

Dhonukshe P, Mathur J, Hülskamp M and Gadella TWJ (2005) Microtubule plus-ends reveal essential links between intracellular polarization and localized modulation of endocytosis during division-plane establishment in plant cells. BMC Biology 3(11).

Dixit R, and Cyr R (2004) Encounters between dynamic cortical microtubules promote ordering of the cortical array through angle-dependent modifications of microtubule behavior. The Plant Cell 16:3274–3284

Dixit R, Chang E and Cyr R (2006) Establishment of polarity during organization of the acentrosomal plant cortical microtubule array. Mol Biol Cell 17(3):1298-1305

Gleeson L, Squires S, and Bisgrove SR (2012) The microtubule associated protein END BINDING 1 represses root responses to mechanical cues. Plant Science 187: 1-9.

Gutierrez L, Mauriat M,Guénin S, Pelloux J, Lefebvre JF, Louvet R, Rusterucci C, Moritz T, Guerineau F, Bellini C, Van Wuytswinkel O. (2008) The lack of a systematic validation of reference genes: a serious pitfall undervalued in reverse transcription-polymerase chain reaction (RT-PCR) analysis in plants. Plant Biotechnology Journal 6(6):609-618.

Ishida T, Kaneko Y, Iwano M, and Hashimoto T (2007) Helical microtubule arrays in a collection of twisting tubulin mutants of Arabidopsis thaliana. Proc Natl Acad Sci U S A. 104(20):8544–8549

Jiang K, Toedt G, Montenegro Gouveia S, Davey NE, Hua S, van der Vaart B, Grigoriev I, Larsen J, Pedersen LB, Bezstarosti K, Lince-Faria M, Demmers J, Steinmetz MO, Gibson TJ, Akhmanova A. (2012) A Proteome-wide screen for mammalian SxIP motif-containing microtubule plus-end tracking proteins. Curr Biol 22(19):1800-7.

Nakamura M, Naoi K, Shoji T, and Hashimoto T (2004) Low concentrations of propyzamide and oryzalin alter microtubule dynamics in Arabidopsis epidermal cells. Plant Cell Physiol 45(9):1330-4.

Okada K. and Shimura Y (1990) Reversible root tip rotation in Arabidopsis seedlings induced by obstacle-touching stimulus. Science 250:274-276.

Shaw SL, Lucas J (2011) Intrabundle microtubule dynamics in the Arabidopsis cortical array. Cytoskeleton (Hoboken) 68(1):56-67.

Squires S and Bisgrove SR (2013) The microtubule associated protein END BINDING1, auxin, and root responses to mechanical cues. J. Plant Growth Regul In press.

Vaughn LM, Baldwin KL, Jia G, Verdonk JC, Strohm AK, Masson PH (2011) The cytoskeleton and root growth behavior. Advances in Plant Biology. B. Liu. New York, Springer. 2:307-326.

4. The Microtubule Associated Protein END BINDING1 Represses Root Responses to Mechanical Cues

A version of this chapter has been published in Plant Science (May 2012, Volume 187, Pages 1–9). Authors include Laura Gleeson, Shannon Squires, and Sherryl Bisgrove.

4.1. Introduction

Plants depend on their root systems for survival; they anchor the plant in place and provide surfaces across which water and minerals are absorbed. To accomplish these functions, roots are able to penetrate through the soil and direct their growth towards locations where conditions are optimal. Mechanical stimulation is one cue that roots continuously respond to as they wind their way around rocks and other debris in the environment. When a growing root tip encounters an impenetrable object, crosstalk between the touch and gravity sensory systems cause the root to adopt a pattern of growth that allows it to maneuver around the obstacle [1]. How roots sense and respond to mechanical stimulation and how these signals modulate gravitropism are active areas of investigation (reviewed in [1, 2]). A number of studies have provided evidence that links Ca^{2+} signaling and plant responses to mechanical cues. Transient increases in cytosolic Ca^{2+} levels as well as changes in the expression of gene products with possible roles in Ca^{2+}-mediated signaling pathways have been measured following mechanical stimulation [1, 3-5].

Analyses of roots growing down along the surface of vertically oriented or reclined agar plates are also providing information about the molecular mechanisms that mediate root responses to mechanical cues and gravity. Under these conditions, roots adopt patterns of growth that reflect their responses to combinations of touch and gravity

cues. They often grow in a waving pattern that is angled or skewed towards one side rather than growing towards the bottom of the plate and they occasionally form loops or coils [6-8]. These growth patterns appear to result from interactions between the root tip and the agar surface. On reclined plates, the agar surface presents a barrier that mechanically impedes the root. Downward growth in response to gravity causes the root tip to continuously push against the agar surface and the resulting mechanical cues cause roots to form waves and loops and to skew as they grow [1, 9].

Several Arabidopsis mutants that exhibit altered patterns of growth on the surface of agar plates have been identified [6, 8, 10-21]. A variety of phenotypes that include alterations to the amount of root waving, skewing, or looping have been observed in different mutants. The relevant genes encode proteins with roles in gravitropism, auxin- or ethylene-mediated responses, signaling pathways, cell wall modification, as well as microtubule organization and/or function. Skewing also varies amongst different wild type accessions of Arabidopsis, a feature that was recently used to identify quantitative trait loci (QTL) that contribute to root skewing behaviors [19, 22]. Although numerous proteins have been identified that appear to have roles in root responses to mechanical cues, the network of interactions that is involved is likely to be complex and defined regulatory pathways have not yet emerged (reviewed in [1, 6, 8, 19, 23].

Prominent amongst the proteins found to modulate root growth on agar surfaces are those associated with the microtubule cytoskeleton. Treatments or mutations that disrupt microtubules cause roots to twist into helices and, when grown on the surface of reclined plates, skewing is enhanced [19, 24]. Arabidopsis seedlings carrying mutations in the gene coding for the microtubule associated protein EB1 also have roots that skew and tend to form more loops than wild type when grown on the surface of vertically oriented or reclined agar plates. However, *eb1* roots are not excessively twisted when compared to wild type plants [11], suggesting that EB1 modulates looping and skewing in a way that is mechanistically different from the proteins that regulate root twisting.

The EB1 family belongs to a group known as +TIPs because they preferentially associate with the more active plus ends of microtubules [25]. Numerous studies in animal and fungal cells have shown that +TIPs form a diverse group of proteins that

have many different functions in cells. They modify actin arrays, participate in signaling pathways, regulate microtubule growth and depolymerization (dynamics), and link microtubules with other structures in the cell [26-28]. From these studies, EB1 family members have emerged as key regulatory +TIPs because they bind directly to microtubule ends, modify microtubule dynamics, and interact with a diverse array of additional proteins [26]. Like their animal and fungal counterparts, plant EB1 proteins preferentially accumulate on growing microtubule ends where they regulate microtubule dynamics [11, 29-32]. Presumably, they also recruit other proteins to microtubules, although plant-specific proteins that interact with EB1 are largely unknown [25]. Based on their roles as core regulatory +TIPs in animals and fungi, EB1 family members have been put forward as candidates for proteins that could relay developmentally relevant information between microtubules and other proteins or structures in cells [23].

The Arabidopsis genome contains three genes coding for EB1 family members, *EB1a* (At3g47690)*, EB1b* (At5g62500)*,* and *EB1c* (At5g67270) [33-35]. The EB1a and EB1b proteins bind microtubule plus ends in mitotic and elongating interphase cells while EB1c is sequestered in the nucleus during interphase and is thought to function primarily on microtubules in mitotic arrays [11, 29-32, 36]. Analyses of mutant phenotypes indicate that EB1b has roles in root responses to touch and/or gravity signals [11]. Arabidopsis plants carrying T-DNA insertions in the *EB1b* gene have roots that exhibit delays in downward bending after encountering obstacles. Mutant roots also exhibit levels of skewing and looping that are substantially higher than wild type plants when grown on the surface of reclined agar plates. Mutants homozygous for either the *eb1b-1* allele in the Wassilewskija (Ws) accession or the *eb1b-2* allele in Columbia-0 (Col-0) exhibit defects in their responses to touch/gravity cues [11]. Mutants carrying a third allele, *eb1b-3* in Col-0, have roots that do not skew when grown on vertically oriented plates, a treatment that provides only minimal levels of mechanical stimulation [30]. This result is consistent with our unpublished observations for *eb1b-2* mutants growing on vertically oriented agar plates. The effects of higher levels of mechanical stimulation on root growth of *eb1b-3* mutants have not been reported. Taken together, the mutant phenotypes indicate that EB1b proteins modulate root responses to combinations of touch and gravity cues, but whether they primarily affect root responses to mechanical cues, gravity, or both was not determined.

Here we report that EB1b represses root responses to mechanical cues. We also find that *eb1b* mutants are hypersensitive to increases in mechanical stimulation, indicating the presence of another competing process that activates the response. Two approaches were taken. 1) The effects of altering the type and amount of mechanical stimulation on *eb1b-1* and wild type (Ws) roots were determined. 2) Root responses to mechanical cues were assessed in double mutants that have mutations in *EB1b* and *PHOSPHOGLUCOMUTASE (PGM), ALTERED RESPONSE TO GRAVITY1 (ARG1),* or *TOUCH3 (TCH3),* genes that encode proteins involved in gravity sensing, signaling, or touch responses respectively. Results from both approaches support a model in which EB1b dampens root responses to mechanical cues and enhances gravitropism while another competing pathway promotes touch-mediated growth

4.2. Materials and methods

4.2.1. Plant material and growth conditions

Seeds corresponding toWassilewskija (Ws), Columbia-0 (Col-0), *pgm-1*, *arg1-3* (SALK_024542) and two lines carrying T-DNA insertions in the *TCH3* gene (SALK_098779 and SALK_122731) were obtained from The Arabidopsis Information Resource (TAIR; http://www.Arabidopsis.org/). The SALK T-DNA Express database, http://signal.salk.edu/cgi-bin/tdnaexpress, [37] was searched to identify putative *tch3* T-DNA insertional mutants. Two lines were chosen for analysis, SALK_098779 and SALK_122731. In SALK_098779, the T-DNA sequence is inserted upstream of the translational start codon and RT-PCR analyses revealed the presence of full-length transcripts in plants homozygous for the T-DNA insertion. Therefore, this line was not analyzed further. The *eb1b-1* allele was previously characterized by Bisgrove et al. [11]. Seeds were sterilized using the vapor phase method [38] and placed on the surface of 0.8% (w/v) or inside 1.0% (w/v) agar (Phytablend, Caisson Laboratories Inc.) plates. Agar medium also contained half-strength Murashige and Skoog (MS; Sigma-Aldrich) supplemented with 0.05 % (w/v) 2-(N-morpholino) ethanesulfonic acid (MES; Sigma-Aldrich) and 1% (w/v) sucrose, pH 5.8. Plates containing seeds were incubated at 4°C for 3 d then grown for 7-9 d at 20°C with a 16-h-light/8-h-dark cycle.

Transgenic *eb1b-1* plants expressing full-length gene products from *EB1b* genes under the control of native regulatory sequences (*eb1b-1 pEB1b:EB1b*) were generated as follows. The full-length *EB1b* gene plus 1.5-kb of sequence upstream of the EB1b start codon in the pCAMBIA1300 vector [32] was used as a template in PCR reactions with the following primers: EB1b 2F 5'-GGGGACAAGTTTGTACAAAAAAGCAGGCTYY AAGCTTCTCCTCTTTTTCTTTGTTT-3'and EB1b 1R 5'-GGGGACCACTTTGTACAAGA AAGCTGGGTYTTCTCCTTTACTCATGGCTCC-3'. The resulting sequence was recombined into the GATEWAY pDONR™ vector (Invitrogen), verified by DNA sequencing, and recombined into the binary vector pMDC99 [39]. This construct was introduced into the *Agrobacterium tumefaciens* strain LBA4404 (Invitrogen) which was then used to transform homozygous *eb1b-1* mutants by the floral dip method [38]. Transformed plants were selected by germinating seedlings on agar plates containing 25 mg/l hygromycin. T2 seeds from hygromycin-resistant T1 plants were tested for segregation on hygromycin plates. Seeds were collected from individual hygromycin-resistant T2 plants belonging to lines that segregated 3 hygromycin resistant seedlings to 1 sensitive and tested for segregation on hygromycin plates. Root responses to mechanical cues were assayed on seedlings from T3 lines that were 100% hygromycin resistant.

4.2.2. Phenotypic and Statistical Analyses

Seedlings were photographed using QCapture Pro software and a Qimaging Retiga 4000R digital camera mounted on an Olympus SZX16 stereo microscope. Measurements were made using either Photoshop or ImageJ software (http://rsbweb.nih.gov/ij/index.html). Statistical analyses (Tukey's tests) were performed using JMP 7 software.

4.2.3. Extraction of nucleic acids

DNA was extracted from leaves using a modification of the protocol outlined in [40]. Frozen tissue was ground and DNA was extracted in a buffer containing 200mM Tris CL (pH 8), 250mM NaCl, 25mM EDTA, 0.5% sodium dodecyl sulfate (SDS). After a low speed (400-900 g) 10 min. centrifugation, an equal volume of cold isopropanol was added to the supernatant and samples were centrifuged again for 5-10 min. at 4°C. The

pellet was washed with 500µl of cold 70% ethanol and centrifuged at 16000 g for 5 min. The supernatant was discarded and the pellet was resuspended in 50µl elution buffer (Qiagen). RNA was extracted from 7-11 day old seedlings using the RNeasy kit (Qiagen). RNA was reverse transcribed using RevertAid Minus First Strand cDNA Synthesis kit (Fermentas) and the oligo (dT) primers provided in the kit. The resulting cDNA was subjected to PCR amplification using the following primers: U (forward) 5'-CCGTGATGTTTTCCCT-3', U (reverse) 5'-CGGAGCTCATTCACGG-3', F (forward) 5'-CCTCGGTAAAAACCGGACA-3', F (reverse) 5'-ACAGCGCTTCGAACAAATCT-3', D (forward) 5'-AAGGTCAGGGTCAAGTGCAG-3', D (reverse) 5'-ACAGCGCTTCGAA CAAATCT-3', EB1b F 5'-GCTTCTCCGTCCTTTTCTCTGCTTCAGTT-3', EB1b R 5'-TTCGGTTCAGTTCACTGTAAAACCAAAAA-3'.

4.2.4. Genotyping

Progeny from crosses to T-DNA insertional mutants were genotyped by PCR using *Taq*DNA polymerase (Invitrogen) and the following primers: LBa1 (recognizes the T-DNA insertion in *arg1-3* and the *tch3*alleles) 5'-TGGTTCACGTAGTGGGCCATCG-3', *ARG1* (AT1G68370) F 5'-CGATTGAAGCACTCTGTGCCA-3', *ARG1* R 5'-TCTGTT CCGCCTTCTTCTCCC-3' *TCH3* (AT2G41100) F 5'-CCTCGGTAAAAACCGGACA-3', *TCH3* R 5'-ACAGCGCTTCGAACAAATCT-3', JL202 (recognizes the T-DNA insertion in *eb1b-1*) 5'-CATTTTATAATAACGCTGCGGACATCTAC-3', *EB1b* (AT5g62500) F 5'-GCTTCTC-CGTCCTTTTCTCTGCTTCAGTT-3', *EB1b* R 5'-TTCGGTTCAGTTCACTGTAAAACC-AAAAA-3'.

Since the *pgm-1* allele carries a point mutation in the *PGM* gene, a derived Cleaved Amplified Polymorphic Sequences (dCAPS) protocol was used to genotype progeny from crosses to *pgm-1*. dCAPS Finder 2.0 software was used to generate a list of possible restriction enzymes that can detect a single nucleotide difference (corresponding to a point mutation) between the wild-type and mutant sequences (http://helix.wustl.edu/dcaps/dcaps.html;[41]. To detect the difference between wild type (Col-0) and *pgm-1* genotypes, the following primers were used to PCR amplify the *PGM* gene from both wild type and *pgm-1*: *PGM* (AT5G51820) F 5'-TTGGATGA-TTTACAATGCTGAAAGA-3', *PGM* R 5'-TCAGTGATCACGAAGGAAAAACTT-3'. The PCR products were digested with the restriction enzyme BspCNI (recognition site:

CTCAG $(N)_9$). Only *pgm-1* contained the BspCNI restriction site due to the point mutation in the *PGM* gene.

4.3. Results

4.3.1. eb1b-1 mutants are hypersensitive to increases in mechanical stimulation

To assess *eb1b-1* responses to mechanical cues, root growth was analyzed in seedlings grown on the surface of tilted agar plates (Fig. 1). Roots growing along the surface of an agar plate are mechanically stimulated by contact between the root tip and the agar surface [7, 9]. When plates are reclined from vertical towards a more horizontal orientation (a higher angle), the amount of mechanical stimulation perceived by the growing root is increased (Fig. 1). On plates oriented at 20°, both wild type (Ws) and *eb1b-1* roots formed loops, although the proportion of roots that made loops was significantly higher for *eb1b-1* (0.19) than it was for wild type (0.04; P=0.006), indicating that EB1b has an inhibitory effect on loop formation. At 35°, both wild type and *eb1b-1* formed more loops than they did at 20°; the proportions of roots that made loops increased to 0.22 for wild type and 0.58 for *eb1b-1* at the higher plate angle, representing increments of 0.18 and 0.39 respectively. The increase in the proportion of roots that made loops was significantly greater for *eb1b-1* than it was for wild type (P=0.036), indicating that *eb1b-1* roots are hypersensitive to the additional mechanical cues provided when seedlings are grown on plates reclined at higher angles.

That EB1b represses root responses to mechanical cues was verified by assessing the proportions of roots that formed loops in mutants transformed with wild type copies of the *EB1b* gene. Transgenic *eb1b-1* plants expressing full-length *EB1b* under the control of 1.5 kb of native upstream regulatory sequences (*eb1b-1 pEB1b:EB1b*) [32] were generated and the proportions of roots that formed loops in transgenic lines were compared to that of wild type (Ws) and *eb1b-1* mutants. In seedlings grown on agar plates reclined by 45º to provide high levels of mechanical stimulation, loop formation in transgenic *eb1b-1* seedlings was reduced from the high levels observed in untransformed mutants to that of wild type or lower (Fig. 1f). Reported here is the data from one transgenic line, although the same phenomenon was also

observed in two additional lines from independent transformation events. The ability of the *EB1b* transgene to reduce looping in mutant roots supports the conclusion that EB1b represses root responses to mechanical cues.

4.3.2. eb1b-1 roots have delayed responses to gravity when grown inside the agar

The analysis of seedlings growing on the surface of tilted plates indicated that *eb1b-1* roots are hypersensitive to mechanical stimulation imposed by the agar surface. To determine whether mutant roots also have growth defects when mechanical cues are evenly distributed, roots grown inside the agar medium were analyzed (Fig. 2). Under these conditions, both wild type and *eb1b-1* roots grew straight down instead of skewing off to one side as they do when grown on the surface. To address the possibility that mutants may have defects responding to gravity when grown inside the agar, plates containing 7 day-old seedlings were rotated 90° in the clockwise direction and roots were observed after they formed a downward bend. The position of the root tip at the time of the reorientation was marked and 2 days later the distance between the mark and the position of the gravitropic bend was measured (Fig. 2e-h). This distance was divided by the growth rate to determine the time each root took to form a bend. The *pgm-1* mutant was used as a positive control because these mutants have gravitropic defects. In wild-type roots, the gravity-sensing columella cells contain starch-filled amyloplasts that trigger a signal when they sediment onto the bottom of the cell in response to gravity [42]. *pgm-1* amyloplasts are starch-deficient because they lack phosphoglucomutase, an enzyme in the starch biosynthetic pathway. This defect results in slower amyloplast sedimentation rates and delays in gravitropic bending [43, 44]. When *pgm-1* roots were grown inside the agar, the time taken to form a bend after a gravity signal was significantly greater for *pgm-1* (24 h) than it was for wild type (Col-0; 12.8 h), indicating that the assay did detect gravitropic defects. Like *pgm-1,* analysis of *eb1b-1* roots took longer (21.1 h) than wild type (Ws; 17.9 h) to form a bend, revealing that gravitropic responses were also delayed in *eb1-1* mutants ($P < 0.01$).

4.3.3. Double mutant analyses

The results reported above indicate that EB1b represses looping and skewing and enhances gravitropism in response to mechanical cues. To further investigate the role of EB1b in touch-and gravity-mediated root growth, *eb1b-1* was crossed to plants carrying mutations in genes associated with responses to either mechanical cues or gravity. Three genotypes were chosen; two mutants, *pgm-1* and *arg1-3*, have defects responding to gravity while the third carries a T-DNA insertion in *TCH3,* a gene that is up- regulated in response to mechanical cues [43, 45, 46]. These mutants exist in Col-0, an accession in which the skewing and looping of roots is strongly attenuated [17]. Although there are *eb1b* mutant alleles available in the Col-0 genetic background [11, 30], the reduced responses to mechanical cues observed in this accession make it difficult to analyze the effects of mechanical cues on mutant phenotypes. *eb1b-2* mutants (in Col-0) have roots that skew significantly more than wild type Col-0 when grown on reclined agar surfaces [11], but the difference is not large enough to discern intermediate responses without analyzing prohibitively large numbers of seedlings. Since we were interested in investigating the effects of both strong and mild levels of mechanical stimulation as well as possible intermediate phenotypes in double mutants, we used *eb1b-1* mutants in Ws for our crosses. Azygous wild type as well as homozygous single and double mutants in the Ws/Col-0 background were identified from the progeny of the crosses and used in our assays. All genotypes were verified using a PCR-based protocol to detect the presence or absence of T-DNA insertional alleles corresponding to the *eb1b-1, arg1-3,* and *tch3-1* mutations. A dCAPs protocol was used to detect the presence or absence of the point mutation corresponding to the *pgm-1* allele (see Materials and Methods for details). A comparison of the responses of homozygous wild type and *eb1b-1* progeny isolated from the three separate crosses provides evidence that the mixed Ws/Col-0 background in the progeny is not interfering with our analysis of the *eb1b-1* phenotype (Figs. 3i, 3j, 4e, 4f, 6h, and 6i). In all cases, roots of *eb1b-1* mutants skewed and looped to an extent that was far greater than the variability observed between wild type lines derived from separate crosses.

To assay root responses to mechanical cues, two measurements were made on seedlings that were grown on the surface of either vertically oriented or reclined plates. (1) The angle between the gravity vector and the root tip (skewing angle or ɵ, Fig 3 a)

was measured on seedlings growing on vertically oriented plates. A vertical plate orientation was chosen as a treatment that would provide mild mechanical stimulation. Skewing angles were measured because roots rarely form loops under these conditions. (2) The proportion of roots with loops was determined from seedlings grown on plates oriented at 45°, a condition that provides substantially higher levels of mechanical stimulation causing many roots to form loops.

4.3.4. Root responses to mechanical cues in eb1b-1 pgm-1 double mutants

As discussed previously, *PGM* encodes an enzyme that is required for starch biosynthesis. Without starch, amyloplasts in the root cap columella cells sediment at a slower rate in response to gravity resulting in delays in gravitropic bending [43, 44]. On vertical plates, skewing of *pgm-1* and wild type roots was statistically indistinguishable (Fig. 3). However, both *eb1b-1* and *eb1b-1 pgm-1* skewed more than wild type or *pgm-1* and the skewing angles of double mutants were statistically indistinguishable from *eb1b-1*, suggesting that the *pgm-1* mutation has little to no effect on root skewing when seedlings are grown on vertically oriented plates, possibly because the amount of gravistimulation provided under these conditions is negligible. In contrast, *pgm-1* grown on 45° plates exhibited a higher frequency of roots with loops than did wild type, a result that is consistent with a previous report that roots of the *pgm* mutant TC75 tend to form loops when grown on reclined plates [47]. Although the proportion of *pgm-1* roots with loops was greater than wild type, it was less than that of *eb1b-1*. In double mutants, the proportion of roots that formed loops was slightly higher than it was for *eb1b-1*, although the difference was not statistically significant (P=0.0685). A double mutant phenotype that is equivalent to *eb1b-1* suggests that *EB1b* and *PGM* affect the same process. However, we cannot rule out the possibility of a slight additive effect in the double mutants.

4.3.5. Analyses of eb1b-1 arg1-3 double mutants

ARG1 encodes a DnaJ-like protein that is also involved in root responses to gravity but in a pathway that is genetically distinct from *PGM* [46, 48, 49]. In response to a change in plant orientation within the gravity field, *arg1* mutants have defective

relocalization of PIN3, an auxin efflux carrier that directs auxin movement through the columella cells in the root cap. The mutants also have delayed responses to gravitropic cues [46]. To further explore possible genetic interactions between *EB1b* and genes involved in gravity responses, the progeny of crosses between *eb1b-1* and *arg1-3* were analyzed. As was observed in the experiments described above, *eb1b-1* roots skewed more when grown on vertically oriented plates and a higher proportion formed loops than did wild type or *arg1-3* on reclined plates (Fig 4). *arg1-3* roots skewed less than wild-type, although it is not clear whether this difference is relevant since it is no larger than the variability seen between different Ws/Col-0 wild type lines. However, the *eb1b-1 arg1-3* mutants displayed skewing angles that were substantially lower than *eb1b-1*, suggesting that the *eb1b-1* phenotype is suppressed in the *arg1-3* mutant background. A similar result was observed when loop formation was assessed in seedlings grown on plates oriented at 45°. Although the proportion of loops formed by *arg1-3* was similar to that of wild-type, the proportion of loops formed in the double mutants was less than *eb1b-1* and greater than *arg1-3.* In both cases, the differences observed between *eb1b-1* and the *eb1b-1 arg1-3* double mutants were larger than the variability observed between different Ws/Col-0 wild type lines. Taken together, the phenotypes of *eb1b-1 arg1-3* double mutants suggest that the *eb1b-1* phenotype is suppressed in the *arg1-3* mutant background. Since both *eb1b-1* and *arg1-3* are recessive [11, 49], it is also possible that the two genes have opposing and additive effects on looping and skewing.

4.3.6. Molecular characterization of T-DNA insertional alleles of TCH3

To investigate genetic interactions between *eb1b* and a putative touch-response mutant, the SALK T-DNA Express database, http://signal.salk.edu/cgi-bin/tdnaexpress, [37] was searched to identify plants with T-DNA insertions in *TOUCH3 (TCH3;* AT2G41100), a gene that is up-regulated in mechanically stimulated plants. *TCH3* encodes a calmodulin-like protein that contains six EF-hand domains and is also known as CML12 [3-5, 50]. The protein is expressed in several tissues and organs including the root cap and elongation zone which correspond to regions of mechanical perception and response [51].

We analyzed a line, SALK_122731, in which the T-DNA is inserted in the final exon of the *TCH3* gene (arrowhead in Fig. 5a). RT-PCR analyses were conducted using mRNA isolated from SALK_122731. As a control to test for the presence of amplifiable cDNA, primers specific for *EB1b* sequences were used in PCR reactions. Products of the appropriate size were amplified from both Col-0 and the SALK line, indicating that cDNA sequences of EB1b were successfully produced in the RT reactions. Three sets of primers that anneal to regions of the *TCH3* cDNA located upstream (U), on either side (flanking; F) or downstream (D) of the T-DNA insertion site were used. Amplicons were detected for Col-0 with all three primer sets. In contrast, amplicons were not observed in samples from the SALK line when the U and F primer sets were used, indicating that full-length transcripts corresponding to the *TCH3* gene were undetectable in these seedlings. Although full-length transcripts were not detected, a band was produced with the D primer set, indicating the presence of truncated transcripts corresponding to sequences on the 3' side of the T-DNA insertion. The downstream transcript corresponds to one of the six EF hand domains present in TCH3 and a start codon is available in a correct reading frame, raising the possibility that this allele may have partial function. However, because our results with the U and F primer sets indicated that full length transcripts are not present, this line was analyzed and the allele was named *tch3-1*.

4.3.7. Gravitropic response of tch3-1 when grown inside the agar

The analysis of *eb1b-1* roots growing inside agar indicated that these mutants have delayed gravitropic responses when mechanical stimulation is evenly distributed (Fig. 2). For comparative purposes, root growth in *tch3-1* mutants was assessed under the same conditions. Seeds were embedded in the agar and the plates were oriented vertically, allowing the roots to grow through the agar. Both wild type (Col-0) and *tch3-1* roots grew straight down. After 7 days plates containing seedlings were rotated 90° in the clockwise direction and the position of the root tip was marked (Fig. 6). After the roots formed a gravitropic bend the distance between the initial position of the root tip and the point where the downward bend formed was measured and divided by the growth rate of the root to determine the time taken to form a bend. In contrast to *eb1b-1, tch3-1* roots took significantly less time to form a bend (9.3 h) than did wild type (Col-0; 11.9 h) indicating that gravitropism is enhanced in this mutant.

4.3.8. tch3-1 mutants are resistant to mechanical cues

In contrast to the hypersensitivity of *eb1b-1*, *tch3-1* mutants are resistant to mechanical stimulation. On both vertical and reclined plates, root skewing angles and the proportions of roots that formed loops were far lower in *tch3-1* single and *eb1b-1 tch3-1* double mutants than they were in *eb1b-1* (Fig. 6), indicating that the *tch3-1* allele eliminates the additional skewing and looping seen in *eb1b-1* mutants. The *tch3-1* roots also skewed less than wild type, although the relevance of this observation is unclear. In contrast to the large difference in skewing angles observed between *eb1b-1* and all other genotypes, the difference between *tch3-1* and wild type is small and falls within the variability seen between different lines of wild type plants isolated from the Ws/Col-0 crosses. In addition, a recently published study did not detect a difference in skewing between another *tch3* T-DNA insertional allele (SALK 090554; *cml12-2*) and wild type Col-0 roots [20]. Regardless of the *tch3-1* phenotype, it is clear that the presence of *tch3-1* alleles in the *eb1b-1 tch3-1* double mutants suppressed the excessive looping and skewing observed in *eb1b-1* single mutants. The differences in both looping and skewing between *eb1b-1* and *eb1b-1 tch3-1* double mutants were far larger than the variability observed between different Ws/Col-0 wild type lines.

Given that *TCH3* gene expression is up-regulated in plants responding to touch [3, 5], the lack of response in *eb1b-1 tch3-1*and *tch3-1* may result from a loss of TCH3 activity if *tch3-1* is recessive. Alternatively, the lack of response may be due to a dominant negative effect of the *tch3-1* allele since we detected a truncated transcript that would encode a protein fragment with a Ca^{2+}-binding domain in homozygous *tch3-1* mutants (Fig. 5). To distinguish between these possibilities progeny from a plant homozygous for *eb1b-1* and heterozygous for *tch3-1* were examined. Seedlings were grown on agar plates reclined at 45º and after 7 days the proportion of roots that formed loops was found to be 0.64 (n = 719 in 5 separate experiments). This number was compared to the proportions expected in a segregating population in which *tch3-1* is either recessive (expected proportion = 0.65) or acting as a dominant negative (expected proportion = 0.45). The expected proportions were calculated from measurements made on *eb1b-1 tch3-1* (n = 189) and *eb1b-1* (n = 251) homozygotes from sibling lines in the same experiments. These results indicate that *tch3-1* is recessive, since the proportion of roots with loops in the segregating population (0.64)

was statistically indistinguishable from the proportion expected if *tch3-1* is recessive (0.65; P = 0.789, χ^2 test) and significantly different from the proportion expected if *tch3-1* was dominant (0.45; P = 0.0002, χ^2 test).

4.4. Discussion

The microtubule plus end binding protein EB1b was previously shown to have a role in root responses to combinations of touch and gravity cues [11], but whether it affected responses to mechanical cues, gravity, or both was not known. The data reported here show that EB1b dampens root responses to mechanical cues and that another competing process activates them.

4.4.1. EB1b represses root responses to mechanical cues

Evidence supporting the conclusion that EB1b represses root responses to mechanical cues comes from the analysis of mechanically-stimulated roots growing on reclined agar plates. We find that *eb1b-1* roots growing on reclined plates make more loops and skew more than wild type. Given that the *eb1b-1* allele is recessive [11], this result suggests that EB1b activity represses touch-induced root phenotypes. The results reported here as well as previously published data [11] have shown that roots of both *eb1b-1* (in the Ws accession) and *eb1b-2* (in Col-0) skew significantly more than wild type when grown on reclined plates [11]. These results are not inconsistent with the observation that roots of *eb1b-3* mutants in the Col-0 accession do not skew when grown on the surface of vertically oriented plates [30], since this is a growth regime that provides only minimal amounts of mechanical stimulation. Another line of evidence indicating that EB1b represses root responses to mechanical cues comes from the analysis of transgenic *eb1b-1* mutants expressing wild type copies of *EB1b* gene products from transgenes. In transgenic lines, looping was significantly reduced from the high levels observed in untransformed mutants to low levels that were equivalent to wild type roots. Taken together, these results indicate that EB1b represses root responses to mechanical cues.

The hypersensitivity of *eb1b-1* mutants to increases in mechanical stimulation indicates the existence of another process that activates root looping and skewing in

response to touch. When plates are reclined at higher angles, both mutants and wild type form more loops. However, the increase observed in *eb1b-1* mutants is greater than that of wild type (Ws), indicating that the mutants are more sensitive to this treatment than wild type. The loss of repressive activities in *eb1b-1* can account for differences in loop formation between mutants and wild type but not the hypersensitivity. The fact that *eb1b-1* roots are hypersensitive to increases in mechanical stimulation suggests the existence of a positive regulatory pathway that activates skewing and looping in response to touch.

Analyses of roots growing inside the agar, a condition that provides uniformly distributed mechanical cues, suggest that EB1b activities enhance gravitropic responses. In comparison to wild type (Ws), mutant *eb1b-1* roots growing through the agar exhibited delays in their response to gravity. Delays in gravitropic bend formation were also reported for *eb1b-1* roots growing on the surface of the media and for roots navigating around a barrier [11]. Noteworthy is the fact that loss of EB1b activity has opposite effects on root looping/skewing and gravitropism. In touch-stimulated *eb1b-1* roots, gravitropic bending is delayed [11] while looping is enhanced (Fig.1), indicating that EB1b activities promote gravitropism and inhibit looping/skewing in roots responding to mechanical cues. Two scenarios that could explain the opposing effects of EB1b on touch and gravity-mediated growth are as follows. 1) The protein could reduce looping and skewing indirectly by reinforcing gravity responses when mechanically stimulated. 2) EB1b could exert opposing effects on each process through different sets of interactions, a possibility supported by the observation that EB1 proteins have many different binding partners in metazoan and fungal cells [52].

4.4.2. Genetic interactions between EB1b and components of gravity and touch signaling pathways.

Analyses of double mutant phenotypes between *eb1b-1* and seedlings with mutations in genes that encode proteins involved in gravity sensing, signaling, or touch responses support a model in which EB1b represses skewing and looping and enhances gravitropism in roots responding to mechanical cues. *EB1b* and *PGM,* a gene involved in gravity sensing, appear to act on the same process. We found that root responses to mechanical cues in *eb1b-1 pgm-1* double and *eb1b-1* single mutants were equivalent,

suggesting that the effects of *PGM* on root responses to mechanical cues may be dependent on *EB1b*. Although the possibility of a small additive effect in double mutants cannot be ruled out, an epistatic relationship between *EB1b* and *PGM* is intriguing, given that the signal promoting gravitropism during amyloplast sedimentation is believed to be mechanical in nature [42] and EB1b promotes gravitropic bending [11].

ARG1, a gene that encodes a protein involved in the transduction of gravity-induced signals, appears to function independently of *EB1b.* Mutation of the *ARG1* gene significantly reduced looping and skewing of *eb1b-1* in double mutants to levels that were intermediate between the *eb1b-1* and *arg1-3* single mutants, indicating that the *eb1b-1* phenotype is suppressed in the *arg1-3* mutant background. Since *eb1b-1* and *arg1-3* are recessive [11, 49], the double mutant phenotype may also represent an additive relationship in which the genes act independently of one another. This possibility is consistent with a scenario in which *EB1b* and *PGM* act in the same process, since *ARG1* appears to function in a branch of the gravitropic signaling pathway that is genetically distinct from *PGM* [48].

The *TCH3* gene has been linked to the activation of plant responses to mechanical stimulation. It is one of twelve genes encoding calmodulin-like proteins that are transcriptionally activated in response to mechanical cues [3, 5]. Calmodulin-like proteins are thought to participate in Ca^{2+}-mediated signal transduction pathways by binding Ca^{2+} and activating downstream targets [1, 4, 53]. We found that *tch3-1* mutants had roots that failed to respond to either mild or high levels of mechanical stimulation, consistent with an inability to activate the response. The same effect was seen in *eb1b-1 tch3-1* double mutants, raising the possibility that the hypersensitivity of *eb1b-1* roots to mechanical cues may be due to unrepressed TCH3 activity. Although we detected the presence of a partial transcript encoding a protein fragment with a single Ca^{2+}-binding domain in *tch3-1* mutants, the allele does not act as a dominant negative since it is recessive.

4.4.3. Roles for EB1b in root responses to touch/gravity cues: A model

We propose that at least two competing processes modulate root responses to mechanical cues. One process activates touch-dependent root growth in response to

mechanical stimulation while the other, in which EB1b is involved, represses touch-mediated responses and enhances gravitropism. When the amount of mechanical stimulation is minimal, as would occur on vertically oriented plates, the outcome would be shifted in favor of gravity-driven downward growth. Additional mechanical cues, such as growth on reclined plates, would enhance output from the positive regulatory pathway thereby tipping the balance towards touch-mediated growth (looping and skewing). One candidate for a protein that could induce touch responses in roots is TCH3, since *TCH3* gene expression is activated in aerial organs in response to mechanical cues [3, 5], the protein localizes to regions of the root involved in mechanical perception and response (root cap and elongation zone) [50], and *tch3-1* mutants are unable to respond to touch stimulation (this report). Whether or how gravity perception /signaling might feed in to such a regulatory network is an interesting question. Our results imply that ARG1 may not play a role in the EB1b-mediated process, because the *eb1b-1 arg1-3* double mutant phenotype is additive. Our analysis of *eb1b-1 pgm-1* double mutants, on the other hand, suggests the corresponding genes may act on the same process, raising the possibility of a link between gravity detection and EB1b.

How might a microtubule +TIP protein like EB1b participate in this kind of regulatory network? Mounting evidence, mainly from studies in animal and fungal cells, suggests that EB1 provides a platform on microtubule ends to which a wide array of proteins with diverse functions is recruited [25, 26, 52]. These include proteins that participate in signaling pathways, an example being adenomatous polyposis coli (APC), a protein involved in β-catenin signaling in mammalian cells. In this example interactions between EB1 and APC interfere with an interaction between β-catenin and APC, thereby allowing β-catenin to accumulate in the nucleus where it regulates transcription [27]. Other interacting partners of EB1 include ion channels as well as proteins that modify the actin cytoskeleton, and in these cases EB1 activity is important for the proper positioning or organization of subcellular components involved in signaling or other cellular activities [54-57]. Whether EB1b functions by interacting with proteins that transmit mechanical cues or by ensuring that the necessary subcellular components are properly positioned within the cell awaits further study.

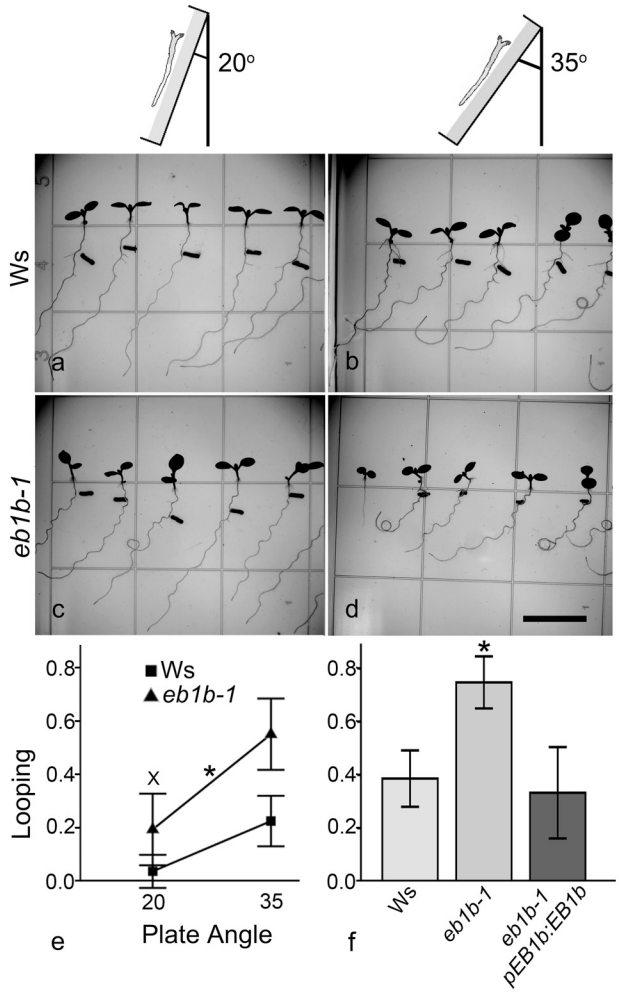

Figure 4.1. The roots of eb1b-1 mutants are more sensitive to growth on reclined agar plates than Ws or eb1b-1 transformed with an EB1b construct (eb1b-1 pEB1b:EB1b).

Roots of Ws (a, b) and *eb1b-1* (c, d) seedlings skew or form loops when grown on plates reclined at either 20° (a, c) or 35° (b, d). For each genotype the average proportion of roots that made loops after 7 days of growth on plates reclined at 20°, 35° (e), or 45° (f) is shown. Size bar in (d) is 1 cm and applies to all photographs. The average proportions of loops made by Ws (squares, n = 94) and *eb1b-1* (triangles, n = 103) from 6 experiments are shown. In (e) the X and the * denote significant differences (Tukey's Test, P = 0.006 and 0.036 respectively). Grey bars in (f) represent the average proportions of loops made by Ws (n = 148), *eb1b-1* (n = 143), and *eb1b-1 pEB1b:EB1b* (n = 130) in 6 experiments and the * denotes a significant difference between *eb1b-1* and the other two genotypes (P < 0.0001, Tukey's test). 95% confidence intervals (CIs) are indicated by black black bars in e and f.

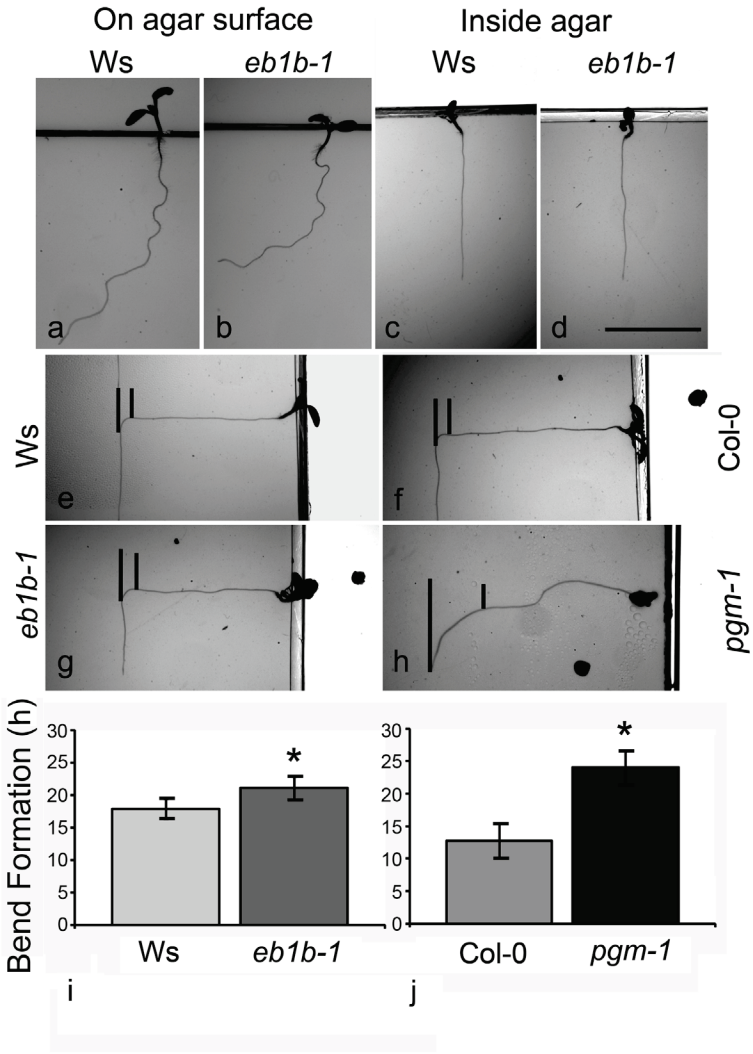

Figure 4.2. Gravitropic responses of eb1b-1 mutants and wild type when grown through an agar medium.

On the surface of vertically oriented plates, roots of 7-day-old *eb1b-1* (b) seedlings skew more than wild type Ws (a) while inside the agar roots of 7-day-old Ws (c) and *eb1b-1* (d) seedlings grow straight down. When 7-day-old seedlings growing inside the agar medium were rotated by 90º in the clockwise direction, Ws (e), Col-0 (f), *eb1b-1* (g) and *pgm-1* (h) roots respond by bending down. The time taken to form a bend was determined by marking root tip position at the time of rotation and the location where root growth became reoriented parallel with the new gravity vector (indicated by vertical lines in the photographs) and this distance was divided by the growth rate. Averages for *eb1b-1* and Ws (i) and for *pgm-1* and Col-0 (j) are shown. Size bar in (d) represents 1 cm and applies to (a) – (h). Grey bars in (i) and (j) represent average distances for seedlings from 4 experiments for Ws and *eb1b-1* (n = 83) and 3 experiments for Col-0 and *pgm-1* (n = 50). Black bars in (i) and (j) represent 95% CIs and the * in (j) denotes a significant difference between *pgm-1* and Col-0 ($P < 0.05$, Tukey's test).

Fig. 3

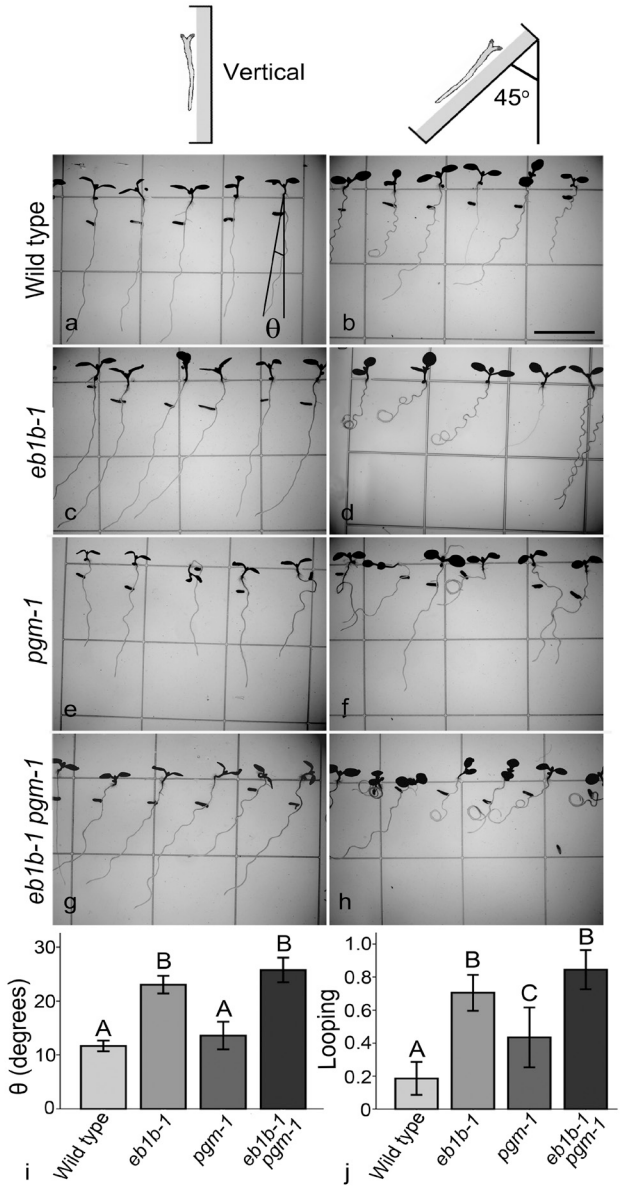

Figure 4.3. Phenotypic analyses of eb1b-1 pgm-1 double mutants.

Wild type (a, b) *eb1b-1* (c, d), *pgm-1* (e, f) and *eb1b-1 pgm-1* (g, h) seedlings were grown on vertically oriented (a, c, e, g) and reclined (b, d, f, h) plates. (i) Average skewing angles were obtained for each genotype by measuring the angle ɵ (shown in a) for roots grown on vertically oriented plates. (j) The average proportions of roots that formed loops (looping) was determined from seedlings grown on plates reclined at 45°. Size bar in (b) represents 1 cm and applies to (a) – (h). Grey bars in (i) and (j) represent averages from 5 experiments (n = 74 - 113 roots for each genotype). Black bars denote 95% CIs. A, B, and C refer to statistically different averages ($P < 0.05$, Tukey's test).

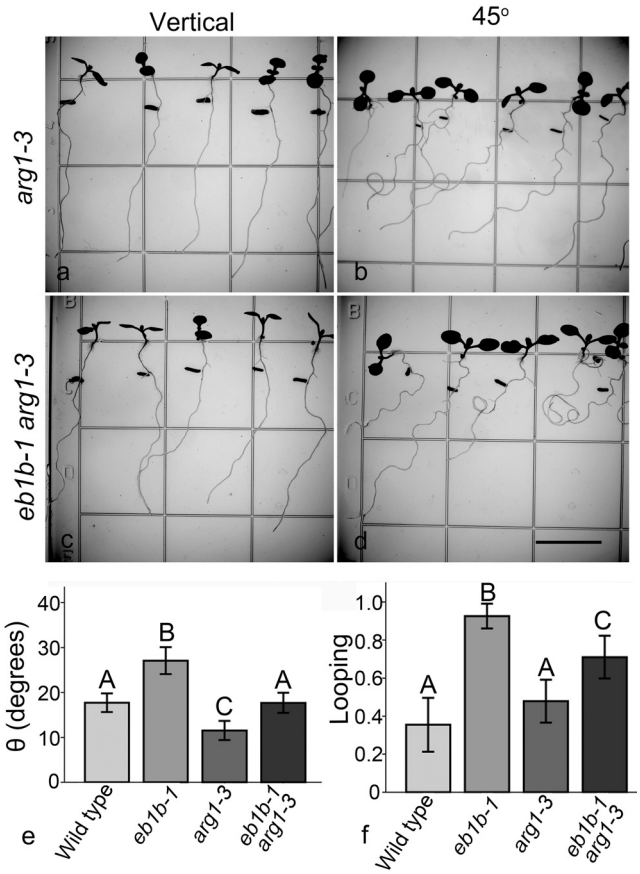

Figure 4.4. Eb1b-1 arg1-3 double mutant roots skewed and looped less than eb1b-1.

Phenotypes of *arg1-3* (a, b) and *eb1b-1 arg1-3* double mutants (c, d) grown on vertically oriented (a, c) and reclined (b, d) plates. Average skewing angles (e) and proportions of roots that formed loops (f) were measured as described in Fig. 3. Size bar in (b) represents 1 cm and applies to (a) – (d). Grey bars in (e) and (f) represent averages from 5 experiments (n = 80 – 120 roots for each genotype). Black bars denote 95% CIs. A, B, and C refer to statistically different averages ($P < 0.05$, Tukey's test).

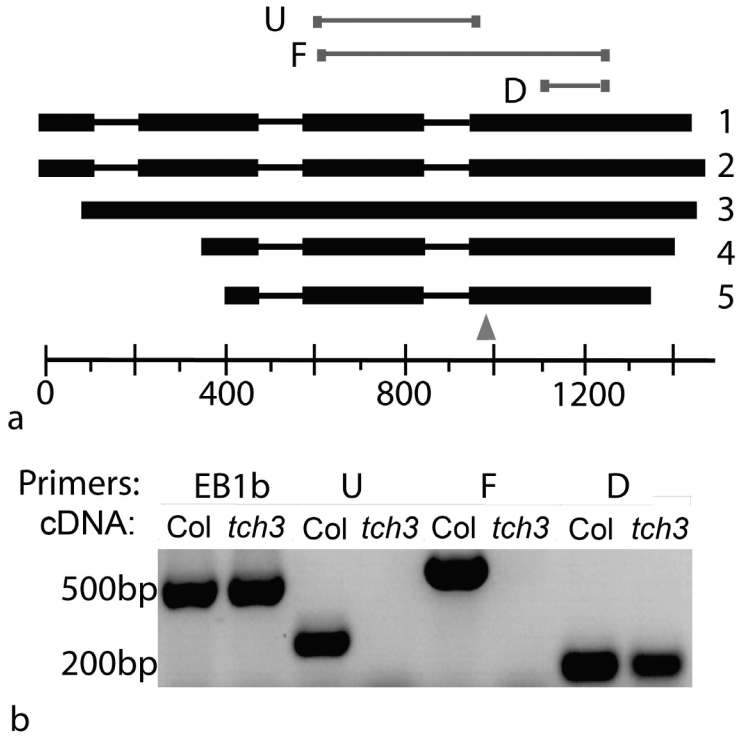

Figure 4.5. RT-PCR analysis of TCH3 T-DNA insertional lines.

(a) A map of the *TCH3* (AT2G41100) locus showing five predicted transcripts (introns represented as black lines and exons as black boxes), binding sites for the U, F, and D primer pairs (small grey boxes) with amplicons between them (grey lines). Grey arrowhead marks the site of the T-DNA insertion in the *tch3-1* allele (SALK_122731). The scale is in nucleotides. (b) RT-PCR analyses using RNA extracted from homozygous *tch3-1* seedlings was analyzed by RT-PCR, an amplicon was detected only in PCR reactions in which the D primer pair was used although amplicons corresponding to *EB1b* sequences were detected in all of the samples. The U, F, and D primer pairs amplified sequences of the appropriate size in cDNA synthesized from wild type Col-0 RNA templates. PCR primer pairs and sources of the RNA templates used in RT reactions are indicated along the top of the gel.

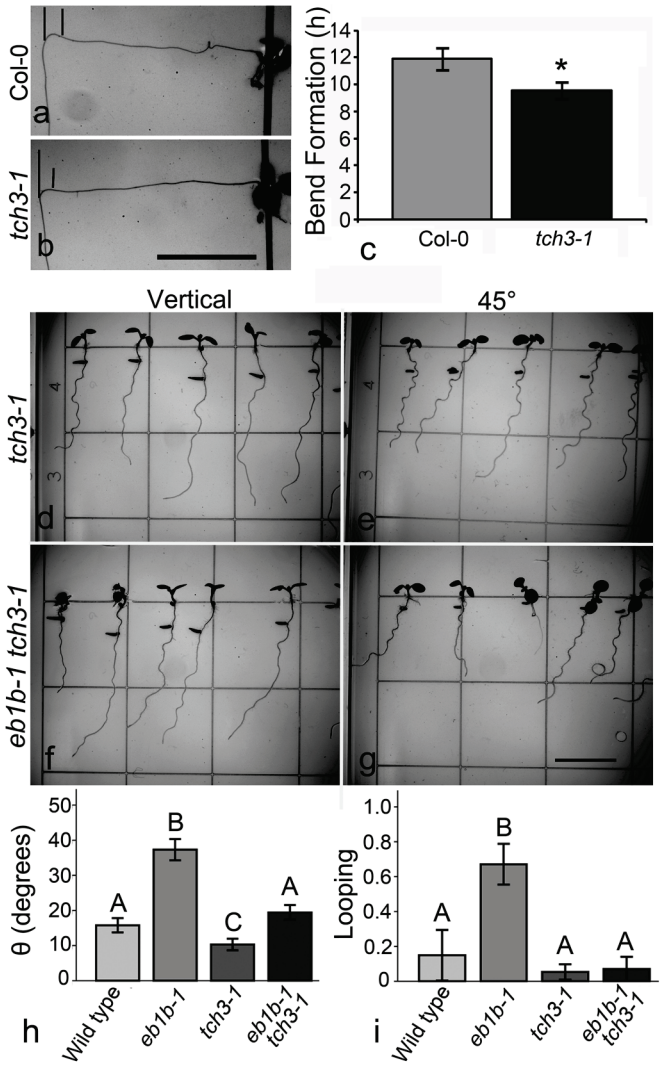

Figure 4.6. Phenotypic analysis of tch3-1 and eb1b-1 tch3-1 seedlings.

When 7 day-old seedlings growing through an agar medium were rotated by 90º in the clockwise direction, wild type Col- 0 (a) and *tch3-1* (b) roots responded by bending down although the time taken to form a bend (c) was less for *tch3-1* than it was for Col-0. Analysis of *tch3-1* (d, e) and *eb1b-1 tch3-1* double mutants (f, g) grown on vertically oriented (d, g) and reclined (e, g) agar plates revealed that *tch3-1* single and *eb1b-1 tch3-1* double mutants had average skewing angles (h) and proportions of roots that formed loops (i) that were equivalent to wild type. Size bars in (b) and (g) represent 1 cm and they also apply to (a) and (d - f) respectively. Vertical lines in (a) and (b) denote the root tip position at the time of rotation and the location where root growth became reoriented parallel with the new gravity vector. Grey bars in (c) represent averages from 3 experiments (n = 80 for Col-0 and n = 115 for *tch3-1*) while those in (h) and (i) represent averages from 6 experiments (n = 119 – 148 or 73 – 92 respectively). Black bars in (c), (h), and (i) represent 95% CIs. A, B, and C refer to statistically different averages ($P < 0.05$, Tukey's test).

4.5. References

[1] G.B. Monshausen, S. Gilroy, Feeling green: mechanosensing in plants, Trends Cell Biol. 19 (2009) 228-235.

[2] C. Coutand, Mechanosensing and thigmomorphogenesis, a physiological and biomechanical point of view, Plant Science 179 (2010) 168-182.

[3] J. Braam, R.W. Davis, Rain-, wind-, and touch-induced expression of calmodulin and calmodulin-related genes in Arabidopsis, Cell 60 (1990) 357-364.

[4] E.W. Chehab, E. Eich, J. Braam, Thigmomorphogenesis: a complex plant response to mechano-stimulation, J. Exp. Bot. 60 (2009) 43-56.

[5] D. Lee, D.H. Polisensky, J. Braam, Genome-wide identification of touch- and darknessregulated Arabidopsis genes: a focus on calmodulin-like and XTH genes, New Phytol. 165 (2005) 429-444.

[6] F. Migliaccio, A. Fortunati, P. Tassone, Arabidopsis root growth movements and their symmetry: Progress and problems arising from recent work, Plant Signal. Behav. 4 (2009) 183-190.

[7] K. Okada, Y. Shimura, Reversible root tip rotation in Arabidopsis seedlings induced by obstacle-touching stimulus, Science 250 (1990) 274-276.

[8] M. Oliva, C. Dunand, Waving and skewing: how gravity and the surface of growth media affect root development in Arabidopsis, New Phytol. 176 (2007) 37-43.

[9] M.V. Thompson, N.M. Holbrook, Root-gel interactions and the root waving behavior of Arabidopsis, Plant Physiol. 135 (2004) 1822-1837.

[10] Z. Andreeva, D. Barton, W. Armour, M. Li, L.-F. Liao, H. McKellar, K. Pethybridge, J. Marc, Inhibition of phospholipase C disrupts cytoskeletal organization and gravitropic growth in *Arabidopsis* roots, Planta 232 (2010) 1263-1279.

[11] S.R. Bisgrove, Y.-R.J. Lee, B. Liu, N.T. Peters, D.L. Kropf, The microtubule plus-end binding protein EB1 functions in root responses to touch and gravity signals in Arabidopsis, Plant Cell 20 (2008) 396-410.

[12] C.S. Buer, M.A. Djordjevic, Architectural phenotypes in the *transparent testa* mutants of *Arabidopsis thaliana*, J. Exp. Bot. 60 (2009) 751-763.

[13] C.S. Buer, G.O. Wasteneys, J. Masle, Ethylene modulates root-wave responses in Arabidopsis, Plant Physiol. 132 (2003) 1085-1096.

[14] H. Buschmann, F. C.O., M. Hauptmann, P. Hutzler, T. Laux, C.W. Lloyd, A.R. Schaffner, Helical growth of the *Arabidopsis* mutant *tortifolia1* reveals a plant-specific microtubuleassociated protein, Curr. Biol. 14 (2004) 1515-1521.

[15] Z. Chen, S. Noir, M. Kwaaitaal, H.A. Hartmann, M.-J. Wu, Y. Mudgil, P. Sukumar, G. Muday, R. Panstruga, A.M. Jones, Two seven-transmembrane domain *MILDEW RESISTANCE LOCUS O* proteins cofunction in Arabidopsis root thigmomorphogenesis, Plant Cell 21 (2009) 1972-1991.

[16] S. Pandey, G.B. Monshausen, L. Ding, S.M. Assmann, Regulation of root-wave response by extra large and conventional G proteins in *Arabidopsis thaliana*, Plant J. 55 (2008) 311-322.

[17] R. Rutherford, P.H. Masson, *Arabidopsis thaliana sku* mutant seedlings show exaggerated surface-dependent alteration in root growth vector, Plant Physiol. 111 (1996) 987-998.

[18] J.C. Sedbrook, D.W. Ehrhardt, S.E. Fisher, W.-R. Scheible, C. Somerville, The Arabidopsis *SKU6/SPIRAL* gene encodes a plus end-localized microtubule-interacting protein involved in directional cell expansion, Plant Cell 16 (2004) 1506-1520.

[19] L.M. Vaughn, K.L. Baldwin, G. Jia, J.C. Verdonk, A.K. Strohm, P.H. Masson, The cytoskeleton and root growth behavior, in: B. Liu (Ed.) Advances in Plant Biology, Springer, New York, 2011, pp. 307-326.

[20] Y. Wang, B. Wang, S. Gilroy, E. Wassim Chehab, J. Braam, CML24 is involved in root mechanoresponses and cortical microtubule orientation in *Arabidopsis*, J. Plant Growth Regul. 30 (2011) 467-479.

[21] C.Y.L. Yuen, J.C. Sedbrook, R.M. Perrin, K.L. Carroll, P.H. Masson, Loss-of-function mutations of *ROOT HAIR DEFECTIVE3* suppress root waving, skewing, and epidermal cell file rotation in Arabidopsis, Plant Physiol. 138 (2005) 701-714.

[22] L.M. Vaughn, P.H. Masson, A QTL study for regions contributing to *Arabidopsis thaliana* root skewing on tilted surfaces, G3: Genes, Genomes, Genetics 1 (2011) 105-115.

[23] S.R. Bisgrove, The roles of microtubules in tropisms, Plant Sci. 175 (2008) 747-755.

[24] T. Hashimoto, Microtubule and cell shape determination, in: B. Liu (Ed.) Advances in Plant Biology, Springer, New York, 2011, pp. 245-257.

[25] R.E. Young, S.R. Bisgrove, Microtubule plus end-tracking proteins and their activities in plants, Springer, New York, 2011.

[26] A. Akhmanova, M.O. Steinmetz, Microtubule +TIPs at a glance, J. Cell Sci. 123 (2010) 3415-3419.

[27] M. Liu, S. Yang, Y. Wang, H. Zhu, S. Yan, W. Zhang, L. Quan, J. Bai, N. Xu, EB1 acts as an oncogene via activating beta-catenin/TCF pathway to promote cellular growth and inhibit apoptosis, Mol. Carcin. 48 (2009) 212-219.

[28] L. Sun, J. Gao, X. Dong, M. Liu, D. Li, X. Shi, J.-T. Dong, X. Lu, C. Liu, J. Zhou, EB1 promotes Aurora-B kinase activity through blocking its inactivation by protein phosphatase 2A, Proc. Natl. Acad. Sci. USA 105 (2008) 7153-7158.

[29] J. Chan, G.M. Calder, J.H. Doonan, C.W. Lloyd, EB1 reveals mobile microtubule nucleation sites in *Arabidopsis*, Nat. Cell Biol. 5 (2003) 967-971.

[30] S. Komaki, T. Abe, S. Coutuer, D. Inze, E. Russinova, T. Hashimoto, Nuclear-localized subtype of end-binding 1 protein regulates spindle organization in Arabidopsis, J. Cell Sci. 123. (2010) 451-459.

[31] J. Mathur, N. Mathur, B. Kernebeck, B.P. Srinivas, M. Hulskamp, A novel localization pattern for an EB1-like protein links microtubule dynamics to endomembrane organization, Curr. Biol. 13 (2003) 1991-1997.

[32] R. Dixit, E. Chang, R. Cyr, Establishment of polarity during organization of the acentrosomal plant cortical microtubule array, Mol. Biol. Cell 17 (2006) 1298-1305.

[33] S.R. Bisgrove, W.E. Hable, D.L. Kropf, +TIPs and microtubule regulation. The beginning of the plus end in plants, Plant Physiol. 136 (2004) 3855-3863.

[34] J. Gardiner, J. Marc, Putative microtubule-associated proteins from the Arabidopsis genome, Protoplasma 222 (2003) 61-74.

[35] R.B. Meagher, M. Fechheimer, The Arabidopsis cytoskeletal genome, in: C.R. Somerville, E.M. Meyerowitz (Eds.) The Arabidopsis Book, American Society of Plant Biologists, Rockville, MD, 2003, pp. 1-26.

[36] D. Van Damme, F.-Y. Bouget, K. Van Poucke, D. Inze, D. Geelen, Molecular dissection of plant cytokinesis and phragmoplast structure: a survey of GFP-tagged proteins, Plant J. 40 (2004) 386-398.

[37] J.M. Alonso, A.N. Stepanova, T.J. Leisse, C.J. Kim, H. Chen, P. Shinn, D.K. Stevenson, J. Zimmerman, P. Barajas, R. Cheuk, C. Gadrinab, C. Heller, A. Jeske, E. Koesema, C.C. Meyers, H. Parker, L. Prednis, Y. Ansari, N. Choy, H. Deen, M. Geralt, N. Hazari, E. Hom, M. Karnes, C. Mulholland, R. Ndubaku, I. Schmidt, P. Guzman, L. Aguilar-Henonin, M. Schmid, D. Weigel, D.E. Carter, T. Marchand, E. Risseeuw, D. Brogden, A. Zeko, W.L. Crosby, C.C. Berry, J.R. Ecker, Genome-wide insertional mutagenesis of *Arabidopsis thaliana*, Science 301 (2003) 653-657.

[38] S.J. Clough, A.F. Bent, Floral dip: a simplified method for *Agrobacterium*-mediated transformation of *Arabidopsis thaliana*, Plant J. 16 (1998) 735-743.

[39] M.D. Curtis, U. Grossniklaus, A Gateway cloning vector set for high-throughput functional analysis of genes in planta, Plant Physiol. 133 (2003) 462-469.

[40] S. Dellaporta, J. Wood, J. Hicks, A plant DNA minipreparation: Version II, Plant Mol. Biol. Rep. 1 (1983) 19-21.

[41] M.M. Neff, E. Turk, M. Kalishman, Web-based primer design for single nucleotide polymorphism analysis, Trends Genet. 18 (2002) 613-615.

[42] M.T. Morita, Directional gravity sensing in gravitropism, Annu. Rev. Plant Biol. 61 (2010) 705-720.

[43] T. Caspar, B.G. Pickard, Gravitropism in a starchless mutant of *Arabidopsis*, Planta 177 (1989) 185-197.

[44] N. Saether, T.-H. Iversen, Gravitropism and starch statoliths in an Arabidopsis mutant, Planta 184 (1991) 491-497.

[45] J. Braam, In touch: Plant responses to mechanical stimuli, New Phytol. 165 (2005) 373-389.

[46] J.C. Sedbrook, R. Chen, P.H. Masson, *ARG1 (Altered Response to Gravity)* encodes a DnaJlike protein that potentially interacts with the cytoskeleton, Proc. Natl. Acad. Sci. 96 (1999) 1140-1145.

[47] C. Simmons, D. Soll, F. Migliaccio, Circumnutation and gravitropism cause root waving in *Arabidopsis thaliana*, J. Exp. Bot. 46 (1995) 143-150.

[48] C. Guan, E.S. Rosen, K. Boonsirichai, K.L. Poff, P.H. Masson, The *ARG1-LIKE2* gene of Arabidopsis functions in a gravity signal transduction pathway that is genetically distinct from the *PGM* pathway, Plant Physiol. 133 (2003) 100-112.

[49] B.R. Harrison, P.H. Masson, *ARL2, ARG1* and *PIN3* define a gravity signal transduction pathway in root statocytes, Plant J. 53 (2008) 380-392.

[50] M.L. Sistrunk, D.M. Antosiewicz, M.M. Purugganan, J. Braam, Arabidopsis TCH3 encodes a novel Ca2+ binding protein and shows environmentally induced and tissue-specific regulation, Plant Cell 6 (1994) 1553-1565.

[51] D.M. Antosiewicz, D.H. Polisensky, J. Braam, Cellular localization of the Ca2+ binding TCH3 protein of Arabidopsis, Plant J. 8 (1995) 623-636.

[52] S. Honnappa, S.M. Gouveia, A. Weisbrich, F.F. Damberger, N.S. Bhavesh, H. Jawhari, I. Grigoriev, F.J.A. van Rijssel, R.M. Buey, A. Lawera, I. Jelesarov, F.K. Winkler, K. Wüthrich, A. Akhmanova, M.O. Steinmetz, An EB1-binding motif acts as a microtubule tip localization signal, Cell 138 (2009) 366-376.

[53] J. Kudla, O. Batistic, K. Hashimoto, Calcium signals: The lead currency of plant information processing, Plant Cell 22 (2010) 541-563.

[54] C. Gu, W. Zhou, M.A. Puthenveedu, M. Xu, Y.N. Jan, L.Y. Jan, The microtubule plus-end tracking protein EB1 is required for Kv1 voltage-gated K+ channel axonal targeting, Neuron 52 (2006) 803-816.

[55] N. Minc, S.V. Bratman, R. Basu, F. Chang, Establishing new sites of polarization by microtubules, Curr. Biol. 19 (2009) 83-94.

[56] S.L. Rogers, U. Wiedemann, U. Hacker, C. Turck, R.D. Vale, Drosophila RhoGEF2 associates with microtubule plus ends in an EB1-dependent manner, Curr. Biol. 14 (2004) 1827-1833.

[57] K. Takahashi, T. Tanaka, K. Suzuki, Directional control of WAVE2 membrane targeting by EB1 and phosphatidylinositol 3,4,5-triphosphate, Cell. Signal. 22 (2010) 510-518.

5. Conclusion

In summary, work presented in this thesis supports a model in which EB1b and auxin act as repressors of root responses to mechanical cues, whereas TCH3 functions as an activator (Fig 1). Chemical and genetic data both suggest that EB1b and auxin inhibit responses to touch via parallel pathways. The inhibition by auxin may occur downstream in a TCH3 pathway.

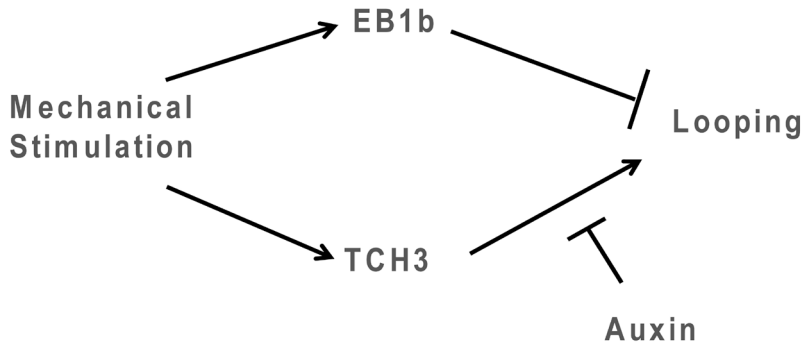

Figure 5.1. A model for the roles of EB1b, auxin, and TCH3 in responses to mechanical cues

EB1b and TCH3 act in opposing pathways to regulate root responses to mechanical stimulation. TCH3 promotes, whereas EB1b inhibits the formation of loops in roots. Auxin acts in parallel with EB1b as an inhibitor of loop formation, and it may carry out its repression by acting on the TCH3 pathway.

The repressive activity of EB1b in responses to touch may depend on its ability to interact with other proteins via its C-terminal domain (Fig. 2a). In an *eb1b-1* mutant (Fig. 2b), or in plants expressing EB1b-GFP (Fig. 2c) the EB1b-interacting protein would be unable to localize to the MT where its activity was required. In contrast, the overexpression of EB1b (Fig 2d) would result in an accumulation of the EB1b binding partner to the MT. The higher concentration of this protein would cause hyper-repression of root responses to touch and result in straighter root growth. Possible candidates for EB1b interacting partners include signaling molecules such as Guanine nucleotide Exchange Factors (GEFs), kinases, or phosphatases.

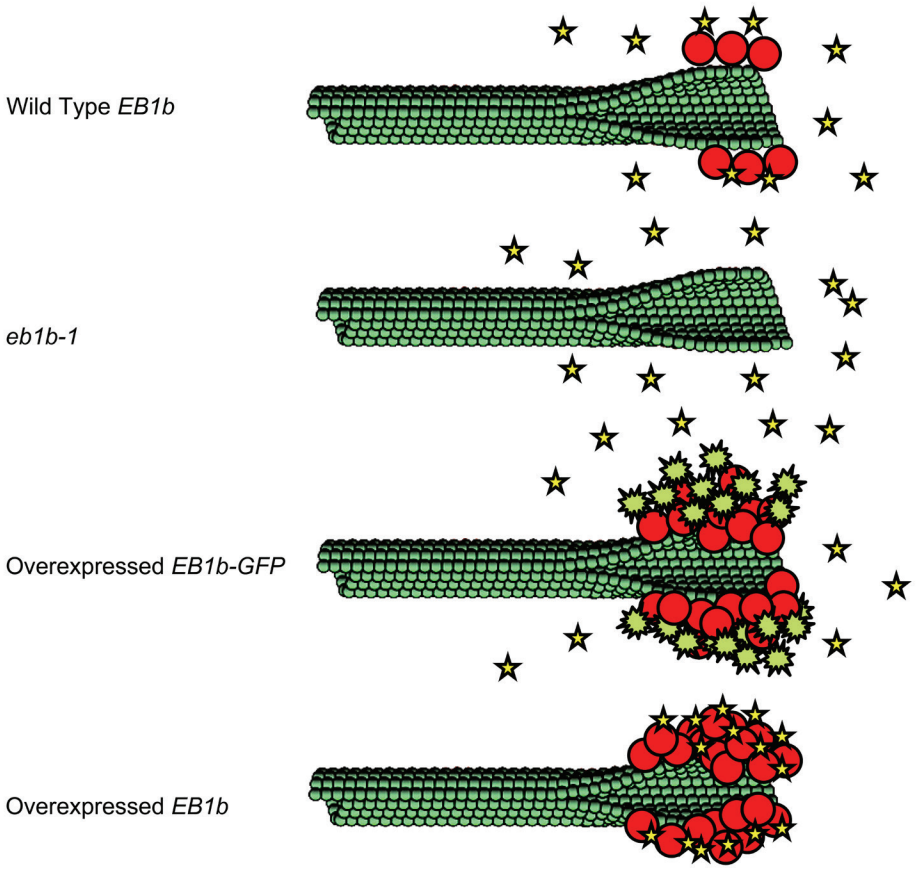

Figure 5.2. A model for the activity of EB1b at the MT plus end.

EB1b (circle, a) may repress root responses to mechanical cues through its interaction with a target molecule (star). This repression could result from the sequestration of an activator, or the localization, and concentration of an inhibitor of responses to mechanical stimuli to the MT plus ends. In the *eb1b-1* mutant (b), or in plants carrying the EB1b-GFP construct (starburst, c), the target molecule is unable to bind EB1b and cannot localize to the MT plus end. The absence of EB1b or its binding partner (star) at the MT plus end results in a hypersensitivity to mechanical cues. Overexpression of functional EB1b (d) would cause the accumulation of the target molecule to the MT and an increase in the EB1b mediated repression of responses to mechanical cues.